The Mode Matching Technique for Electromagnetic Scattering by Inlets With Complex Terminations

Hristos T. Anastassiu and John L. Volakis

Veda Inc.
Suite 200
5200 Springfield Pike
Dayton OH 45431

Wright Laboratory/AARA
Wright-Patterson AFB
OH 45433-7001

October 1993

The Mode Matching Technique for Electromagnetic Scattering by Inlets with Complex Terminations.

Hristos T. Anastassiu John L. Volakis

October 1993

Abstract

The Mode Matching Technique is applied in the evaluation of the Radar Cross-Section of cylindrical inlets terminated by a perfectly conducting cylindrical hub or a cylindrical array of grooves. Closed form expressions are derived for the coupling factors between the various modes. Numerical results are also presented. The purpose of this project is to obtain a reference solution of the problem for validating a Finite Element code for inlet scattering which is currently being developed at the Radiation Laboratory.

1 Introduction

The problem of scattering from cavities is one of the most challenging in applied Electromagnetics. Its significance arises from the fact that one of the most important contributions to the scattered field from aircraft structures is due to engines.

Several attempts have been made so far by various research groups in an effort to characterize the scattering by canonical and irregular cavity configurations. Various methods have been used, but due to the complexity of the problem, crude approximations have to be made, resulting to severe limitations of each technique. Exact analytical procedures, whenever possible, are very cumbersome and inefficient as far as numerical results are concerned.

The most rigorous procedure used in the problem of scattering from inlets with circular cross-section is summarized in [1]. The evaluation of the scattered field is based on the Wiener-Hopf technique, which is only applicable to inlets of circular cross-section and flat terminations. In addition, the resulting mathematical formulas are too complicated for engineering purposes, and consequently the method cannot be used in the analysis of practical inlet configurations.

A formally exact technique used to model waveguide discontinuities, known as the Mode Matching Technique, is described in [2]. As implied by its name, the field is decomposed to a superposition of modes at each side of the discontinuity, and the boundary conditions are used so that the coefficients of the series are calculated. Although the method is rigorous, it can only be used in separable geometries, where mode decomposition is feasible. Moreover, one has to invert an infinite matrix, and problems with the solution are not unusual. Of course, for numerical purposes, only a finite number of modes can be used, but the method is still not efficient for large geometries, where a multitude of propagating modes exist, leading again to a large matrix system.

A combination of a modal technique and high-frequency asymptotic methods, known as the Hybrid Modal Technique, is presented in [3, 4, 5, 6]. The method is based on the evaluation of equivalent currents on the open end and the junctions of the structure. Diffraction effects are also taken into account. This method is usually more efficient than Mode Matching, since no large matrix inversion is necessary, but it is less accurate, since it is only valid for high frequencies. Like Mode Matching, it can be used only in separable geometries and it cannot handle complex terminations. Finally, the method is not readily applicable to inlets having imperfectly conducting walls.

Geometrical Optics (GO) Methods have also been suggested [6] for the same problem. In the context of the Shooting and Bouncing Ray Method (SBR), the incident field is decomposed into a set of parallel ray tubes which are tracked into the cavity via GO laws. Its most significant advantage is the simplicity of the mathematics and implementation. Because of the ray optical assumption, the SBR method is only suitable for large size inlets. In addition, the SBR method does not account for rim diffraction and it suffers from caustic occurance. Some of the disadvantages of the SBR can be eliminated by an improved ray technique, the so-called Generalized Ray Expansion (GRE). In the context of the GRE method the open end aperture is divided into a number of subapartures, and the incident field is decomposed into a set of rays emanating from each subaperture. Unlike the SBR, the rays are not necessarily parallel to each other, and is thus capable in tracing non-planar wavefronts. The method, though, still suffers from limitations inherent to the GO approximation.

Finally, a Gaussian Beam (GB) technique is presented in [6]. The basic idea of this method is the use of Gaussian Beams instead of real rays, so that some of the limitations encountered in SBR and GRE can be overcome. Indeed, real caustics do not exist in this procedure and the incident grid has

to be created only once for all incidence angles. Unfortunately, GO cannot be used very efficiently for GB tracing, since the beams are distorted after each bounce. Moreover, heuristic rules of thumb must be invoked so that the beam characteristics are matched to the geometry. Wide-waisted beams are easier to track, but they may not fit in the cavity aperture, and vice versa.

The most difficult problem encountered in the evaluation of inlet scattering is the mathematical modeling of the termination. In practice, the inlets' termination is the engine's face whose geometrical complexity cannot be handled by any ray optical technique. The current trend is to use the Finite Element Method (FEM) [7] to characterize the fields at the termination. The finite element method is attractive because of its geomerical adaptability and flexibility in modeling materials without a need to alter the the formulation. Moreover, mesh generation packages are available for entering the complex geometry of the engine face. Once the reflected/scattered field from the engine face is known, it can then be traced back to the inlet mouth, from where it radiates in free space.

The goal of this research project is to combine the FEM with other existing techniques, so that the problem of scattering from realistic, jet engine inlets can be solved efficiently. The methodology can be summarized as fol-

lows (see Fig. 1 and 2):

1. The incident field is first tracked from the open end to the termination boundary via modal or GO techniques.

2. The Finite Element Method is then used in conjunction with an artificial absorber for terminating the mesh to evaluate the near zone scattered field from the termination.

3. The scattered field is then integrated over a boundary next to the engine face to yield a corresponding modal or GO representation.

4. The obtained ray optical field is then traced back to the inlet mouth via any of the aforementioned ray techniques.

The validity of the method and the efficiency of the codes have to be tested meticulously, before real problems are attacked. Therefore, the FEM solution has to be compared to reference solutions obtained in simple geometries. The purpose of this report is to show how Mode Matching can be applied to a few such simple geometries, to be used for validating the FEM code.

2 Mode Matching Formulation for a Hollow Cylinder terminated by a Cylindrical Hub

In this chapter we will apply the Mode Matching technique to the geometry of Fig. 3. We assume that a plane wave is incident on the open end of the structure. Our goal is to evaluate the scattered field (and monostatic radar cross section of the structure) as a function of the incidence angle. The following procedure will be applied:

The fields in both regions 1 and 2 can be expressed in terms of waveguide modes, propagating either along the $+z$ or the $-z$ direction. The boundary conditions at the interface between the two regions and at the closed end can be used so that the modes that propagate towards the open end can be expressed in terms of the incident field. Each one of these modes finally radiates in the free space and their superposition yields the scattered field. Diffraction effects from the rim due to outcoming modes are also taken into account.

The geometries of both regions 1 and 2 are separable, therefore Helmholtz's equation can be solved analytically and the fields can be expressed exactly as a superposition of modes. According to [8] the magnetic ($\mathbf{A}^{TM}$) or electric

($\mathbf{F}^{TE}$) vector potentials and the scalar potential Φ^{TEM} corresponding to the modes in each region can be written in the following way:

Region 1.

TM modes:

$$\mathbf{A}^{TM}_{1,np} = \mathbf{u}_z \mu \psi^{TM}_{1,np} \tag{1}$$

where

$$\psi^{TM}_{1,np} = N^{TM}_{1,np} J_n(\gamma^{TM}_{1,np}\rho) \left\{ \begin{array}{c} \sin n\phi \\ \cos n\phi \end{array} \right\} \exp\left\{\pm j\beta^{TM}_{1,np} z\right\} \tag{2}$$

$N^{TM}_{1,np}$ is a normalization factor and $\gamma^{TM}_{1,np}$ is given by

$$J_n(\gamma^{TM}_{1,np} b) = 0 \tag{3}$$

TE modes:

$$\mathbf{F}^{TE}_{1,np} = \mathbf{u}_z \epsilon \psi^{TE}_{1,np} \tag{4}$$

where

$$\psi_{1,np}^{TE} = N_{1,np}^{TE} J_n(\gamma_{1,np}^{TE}\rho) \left\{ \begin{array}{c} \sin n\phi \\ \cos n\phi \end{array} \right\} \exp\left\{\pm j\beta_{1,np}^{TE} z\right\} \tag{5}$$

$N_{1,np}^{TE}$ is a normalization factor and $\gamma_{1,np}^{TE}$ is given by

$$J_n'(\gamma_{1,np}^{TE} b) = 0 \tag{6}$$

Region 2.

TM modes:

$$\mathbf{A}_{2,mq}^{TM} = \mathbf{u}_z \mu \psi_{2,mq}^{TM} \tag{7}$$

where

$$\psi_{2,mq}^{TM} = N_{2,mq}^{TM} B_m(\gamma_{2,mq}^{TM}\rho) \left\{ \begin{array}{c} \sin m\phi \\ \cos m\phi \end{array} \right\} \exp\left\{\pm j\beta_{2,mq}^{TM} z\right\} \tag{8}$$

$$B_m(\gamma_{2,mq}^{TM}\rho) \equiv Y_m(\gamma_{2,mq}^{TM} a) J_m(\gamma_{2,mq}^{TM}\rho) - J_m(\gamma_{2,mq}^{TM} a) Y_m(\gamma_{2,mq}^{TM}\rho) \tag{9}$$

$N_{2,mq}^{TM}$ is a normalization factor and $\gamma_{2,mq}^{TM}$ is given by

$$Y_m(\gamma_{2,mq}^{TM}a)J_m(\gamma_{2,mq}^{TM}b) - J_m(\gamma_{2,mq}^{TM}a)Y_m(\gamma_{2,mq}^{TM}b) = 0 \tag{10}$$

TE modes:

$$\mathbf{F}_{2,mq}^{TE} = \mathbf{u}_z \epsilon \psi_{2,mq}^{TE} \tag{11}$$

where

$$\psi_{2,mq}^{TE} = N_{2,mq}^{TE} G_m(\gamma_{2,mq}^{TE}\rho) \left\{ \begin{array}{c} \sin m\phi \\ \cos m\phi \end{array} \right\} \exp\left\{\pm j\beta_{2,mq}^{TE} z\right\} \tag{12}$$

$$G_m(\gamma_{2,mq}^{TE}\rho) \equiv Y_m'(\gamma_{2,mq}^{TE}a)J_m(\gamma_{2,mq}^{TE}\rho) - J_m'(\gamma_{2,mq}^{TE}a)Y_m(\gamma_{2,mq}^{TE}\rho) \tag{13}$$

$N_{2,mq}^{TE}$ is a normalization factor and $\gamma_{2,mq}^{TE}$ is given by

$$Y_m'(\gamma_{2,mq}^{TE}a)J_m'(\gamma_{2,mq}^{TE}b) - J_m'(\gamma_{2,mq}^{TE}a)Y_m'(\gamma_{2,mq}^{TE}b) = 0 \tag{14}$$

TEM modes:

$$\Phi_2^{TEM} = -N_2^{TEM} \ln\left(\frac{\rho}{b}\right) \tag{15}$$

N_2^{TEM} is a normalization factor.

In all of the above equations,

$$\left(\gamma_{i,jk}^{TM,TE}\right)^2 + \left(\beta_{i,jk}^{TM,TE}\right)^2 = k^2 \tag{16}$$

Also, the normalization factors are arbitrary, but they are usually defined by [5, 9]

$$N_{1,np}^{TM} \equiv \omega\epsilon \left[\frac{1}{2} J_n'\left(\gamma_{1,np}^{TM} b\right) \gamma_{1,np}^{TM} b \sqrt{\pi k Y \beta_{1,np}^{TM} \epsilon_n}\right]^{-1} \tag{17}$$

$$N_{1,np}^{TE} \equiv \left[\frac{1}{2} J_n\left(\gamma_{1,np}^{TE} b\right) \sqrt{\pi k Z \beta_{1,np}^{TE} \epsilon_n \left\{\left(\gamma_{1,np}^{TE}\right)^2 - b^2\right\}}\right]^{-1} \tag{18}$$

$$N_{2,mq}^{TM} \equiv -\frac{\omega\epsilon}{\beta_{2,np}^{TM}} \frac{1}{2} \sqrt{\pi\left(3 - \epsilon_m\right)} \left[\frac{J_m^2\left(\gamma_{2,mq}^{TM} a\right)}{J_m^2\left(\gamma_{2,mq}^{TM} b\right)} - 1\right]^{-\frac{1}{2}} \tag{19}$$

$$\begin{aligned} N_{2,mq}^{TE} \equiv\ & \frac{1}{2}\sqrt{\pi\left(3 - \epsilon_m\right)} \left\{ \left[\frac{J_m'\left(\gamma_{2,mq}^{TE} a\right)}{J_m'\left(\gamma_{2,mq}^{TE} b\right)}\right]^2 \left[1 - \left(\frac{m}{\gamma_{2,mq}^{TE} b}\right)^2\right] - \right. \\ & \left. - \left[1 - \left(\frac{m}{\gamma_{2,mq}^{TE} a}\right)^2\right] \right\}^{-\frac{1}{2}} \end{aligned} \tag{20}$$

$$N_2^{TEM} \equiv \frac{1}{\sqrt{2\pi \ln\left(b/a\right)}} \tag{21}$$

$$\epsilon_n \equiv \begin{cases} 2 & n = 0 \\ 1 & n \neq 0 \end{cases} \tag{22}$$

From the given potentials, the field is obtained from

$$\mathbf{E}_{1,2}^{TM} = -j\omega\mathbf{A}_{1,2}^{TM} + \frac{1}{j\omega\mu\epsilon}\nabla\nabla\cdot\mathbf{A}_{1,2}^{TM} \tag{23}$$

$$\mathbf{E}_{1,2}^{TE} = -\frac{1}{\epsilon}\nabla\times\mathbf{F}_{1,2}^{TE} \tag{24}$$

$$\mathbf{E}_{2}^{TEM} = -\nabla\Phi_{2}^{TEM} \tag{25}$$

The transverse fields are therefore expressed as follows (the longitudinal dependence has been suppressed; **e** stands for the electric and **h** stands for the magnetic field):

Region 1.

$$\begin{aligned}\mathbf{e}_{1,np}^{TM} &= N_{1,np}^{TM}\frac{\beta_{1,np}^{TM}}{\omega\epsilon}\left[\gamma_{1,np}^{TM}J_n'\left(\gamma_{1,np}^{TM}\rho\right)\left\{\begin{array}{c}\sin n\phi\\ \cos n\phi\end{array}\right\}\mathbf{u}_\rho + \right.\\ &+ \left.\frac{n}{\rho}J_n\left(\gamma_{1,np}^{TM}\rho\right)\left\{\begin{array}{c}\cos n\phi\\ -\sin n\phi\end{array}\right\}\mathbf{u}_\phi\right] \qquad (26)\\ \mathbf{h}_{1,np}^{TM} &= N_{1,np}^{TM}\left[\frac{n}{\rho}J_n\left(\gamma_{1,np}^{TM}\rho\right)\left\{\begin{array}{c}\cos n\phi\\ -\sin n\phi\end{array}\right\}\mathbf{u}_\rho - \right.\\ &- \left.\gamma_{1,np}^{TM}J_n'\left(\gamma_{1,np}^{TM}\rho\right)\left\{\begin{array}{c}\sin n\phi\\ \cos n\phi\end{array}\right\}\mathbf{u}_\phi\right] \qquad (27)\\ \mathbf{e}_{1,np}^{TE} &= N_{1,np}^{TE}\left[-\frac{n}{\rho}J_n\left(\gamma_{1,np}^{TE}\rho\right)\left\{\begin{array}{c}\cos n\phi\\ -\sin n\phi\end{array}\right\}\mathbf{u}_\rho + \right.\\ &+ \left.\gamma_{1,np}^{TE}J_n'\left(\gamma_{1,np}^{TE}\rho\right)\left\{\begin{array}{c}\sin n\phi\\ \cos n\phi\end{array}\right\}\mathbf{u}_\phi\right] \qquad (28)\end{aligned}$$

$$\mathbf{h}_{1,np}^{TE} = N_{1,np}^{TE}\frac{\beta_{1,np}^{TE}}{\omega\mu}\left[\gamma_{1,np}^{TE}J_n'\left(\gamma_{1,np}^{TE}\rho\right)\left\{\begin{array}{c}\sin n\phi\\ \cos n\phi\end{array}\right\}\mathbf{u}_\rho + \right.$$
$$\left. + \frac{n}{\rho}J_n\left(\gamma_{1,np}^{TE}\rho\right)\left\{\begin{array}{c}\cos n\phi\\ -\sin n\phi\end{array}\right\}\mathbf{u}_\phi\right] \qquad (29)$$

Region 2.

$$\mathbf{e}_{2,mq}^{TM} = \gamma_{2,mq}^{TM}\left[Y_m\left(\gamma_{2,mq}^{TM}a\right)J_m'\left(\gamma_{2,mq}^{TM}\rho\right) - J_m\left(\gamma_{2,mq}^{TM}a\right)Y_m'\left(\gamma_{2,mq}^{TM}\rho\right)\right]\cdot$$
$$\cdot\ N_{2,mq}^{TM}\frac{\beta_{2,mq}^{TM}}{\omega\epsilon}\left\{\begin{array}{c}\sin m\phi\\ \cos m\phi\end{array}\right\}\mathbf{u}_\rho +$$
$$+\ \frac{m}{\rho}\left[Y_m\left(\gamma_{2,mq}^{TM}a\right)J_m\left(\gamma_{2,mq}^{TM}\rho\right) - J_m\left(\gamma_{2,mq}^{TM}a\right)Y_m\left(\gamma_{2,mq}^{TM}\rho\right)\right]\cdot$$
$$\cdot\ N_{2,mq}^{TM}\frac{\beta_{2,mq}^{TM}}{\omega\epsilon}\left\{\begin{array}{c}\cos m\phi\\ -\sin m\phi\end{array}\right\}\mathbf{u}_\phi \qquad (30)$$

$$\mathbf{h}_{2,mq}^{TM} = \frac{m}{\rho}\left[Y_m\left(\gamma_{2,mq}^{TM}a\right)J_m\left(\gamma_{2,mq}^{TM}\rho\right) - J_m\left(\gamma_{2,mq}^{TM}a\right)Y_m\left(\gamma_{2,mq}^{TM}\rho\right)\right]\cdot$$
$$\cdot\ N_{2,mq}^{TM}\left\{\begin{array}{c}\cos m\phi\\ -\sin m\phi\end{array}\right\}\mathbf{u}_\rho -$$
$$-\ \gamma_{2,mq}^{TM}\left[Y_m\left(\gamma_{2,mq}^{TM}a\right)J_m'\left(\gamma_{2,mq}^{TM}\rho\right) - J_m\left(\gamma_{2,mq}^{TM}a\right)Y_m'\left(\gamma_{2,mq}^{TM}\rho\right)\right]\cdot$$
$$\cdot\ N_{2,mq}^{TM}\left\{\begin{array}{c}\sin m\phi\\ \cos m\phi\end{array}\right\}\mathbf{u}_\phi \qquad (31)$$

$$\mathbf{e}_{2,mq}^{TE} = -\frac{m}{\rho}\left[Y_m'\left(\gamma_{2,mq}^{TE}a\right)J_m\left(\gamma_{2,mq}^{TE}\rho\right) - J_m'\left(\gamma_{2,mq}^{TE}a\right)Y_m\left(\gamma_{2,mq}^{TE}\rho\right)\right]\cdot$$
$$\cdot\ N_{2,mq}^{TE}\left\{\begin{array}{c}\cos m\phi\\ -\sin m\phi\end{array}\right\}\mathbf{u}_\rho +$$
$$+\ \gamma_{2,mq}^{TE}\left[Y_m'\left(\gamma_{2,mq}^{TE}a\right)J_m'\left(\gamma_{2,mq}^{TE}\rho\right) - J_m'\left(\gamma_{2,mq}^{TE}a\right)Y_m'\left(\gamma_{2,mq}^{TE}\rho\right)\right]\cdot$$

$$\cdot \quad N_{2,mq}^{TE} \left\{ \begin{array}{c} \sin m\phi \\ \cos m\phi \end{array} \right\} \mathbf{u}_\phi \tag{32}$$

$$\begin{aligned} \mathbf{h}_{2,mq}^{TE} &= \gamma_{2,mq}^{TE} \left[Y_m' \left(\gamma_{2,mq}^{TE} a \right) J_m' \left(\gamma_{2,mq}^{TE} \rho \right) - J_m' \left(\gamma_{2,mq}^{TE} a \right) Y_m' \left(\gamma_{2,mq}^{TE} \rho \right) \right] \cdot \\ &\cdot \quad N_{2,mq}^{TE} \frac{\beta_{2,mq}^{TE}}{\omega\mu} \left\{ \begin{array}{c} \sin m\phi \\ \cos m\phi \end{array} \right\} \mathbf{u}_\rho + \\ &+ \quad \frac{m}{\rho} \left[Y_m' \left(\gamma_{2,mq}^{TE} a \right) J_m \left(\gamma_{2,mq}^{TE} \rho \right) - J_m' \left(\gamma_{2,mq}^{TE} a \right) Y_m \left(\gamma_{2,mq}^{TE} \rho \right) \right] \cdot \\ &\cdot \quad N_{2,mq}^{TE} \frac{\beta_{2,mq}^{TE}}{\omega\mu} \left\{ \begin{array}{c} \cos m\phi \\ -\sin m\phi \end{array} \right\} \mathbf{u}_\phi \end{aligned} \tag{33}$$

$$\mathbf{e}_2^{TEM} = N_2^{TEM} \frac{1}{\rho} \mathbf{u}_\rho \tag{34}$$

$$\mathbf{h}_2^{TEM} = N_2^{TEM} \frac{1}{Z\rho} \mathbf{u}_\phi \tag{35}$$

The modes which propagate in region 1 towards the open end of the inlet will radiate in free space. The radiated fields in the far zone of the open end are given in Appendix II. If the radiated field of the np outgoing mode of unit amplitude is $\mathbf{E}_{rad}^{TM,TE}(\mathbf{r})$, then it can be shown via reciprocity [3] that given an incident plane wave $\mathbf{E}_{inc}$, the coefficient of the np incoming mode excited by the plane wave is given by

$$a_{np}^{TM,TE} = \frac{2\pi r e^{jkr}}{j\omega\mu} \frac{\mathbf{E}_{inc} \cdot \mathbf{E}_{rad}^{TM,TE}(\mathbf{r})}{\int\int_{S_0} \mathbf{e}_{1,np}^{TM,TE} \times \mathbf{h}_{1,np}^{TM,TE} \cdot d^2\mathbf{S}} \tag{36}$$

where S_0 is the surface of the open end. Using the mode definitions given earlier and the normalizations (17), (18), it follows that

$$\int\int_{S_0} \mathbf{e}_{1,np}^{TM,TE} \times \mathbf{h}_{1,np}^{TM,TE} \cdot d^2\mathbf{S} = 2 \tag{37}$$

The total incident transversal field in region 1 is given by a superposition of modes propagating along the $-z$ direction, i.e.

$$\mathbf{E}_1^{ti} = \sum_{n=0}^{\infty}\sum_{p=1}^{\infty}\left[a_{np}^{TM}\mathbf{e}_{1,np}^{TM}\exp\left\{j\beta_{1,np}^{TM}z\right\} + a_{np}^{TE}\mathbf{e}_{1,np}^{TE}\exp\left\{j\beta_{1,np}^{TE}z\right\}\right] \tag{38}$$

$$\mathbf{H}_1^{ti} = \sum_{n=0}^{\infty}\sum_{p=1}^{\infty}\left[a_{np}^{TM}\mathbf{h}_{1,np}^{TM}\exp\left\{j\beta_{1,np}^{TM}z\right\} + a_{np}^{TE}\mathbf{h}_{1,np}^{TE}\exp\left\{j\beta_{1,np}^{TE}z\right\}\right] \tag{39}$$

The $a_{np}^{TM,TE}$ coefficients are readily evaluated by eq. (36). In a similar manner, the transversal field reflected by the interface back to the open end can be expressed as a superposition of $+z$ propagating modes, namely:

$$\begin{aligned}\mathbf{E}_1^{tr} &= \sum_{n=0}^{\infty}\sum_{p=1}^{\infty}[b_{np}^{TM}\mathbf{e}_{1,np}^{TM}\exp\left\{-j\beta_{1,np}^{TM}z\right\} + \\ &+ b_{np}^{TE}\mathbf{e}_{1,np}^{TE}\exp\left\{-j\beta_{1,np}^{TE}z\right\}]\end{aligned} \tag{40}$$

$$\begin{aligned}\mathbf{H}_1^{tr} &= \sum_{n=0}^{\infty}\sum_{p=1}^{\infty}[-b_{np}^{TM}\mathbf{h}_{1,np}^{TM}\exp\left\{-j\beta_{1,np}^{TM}z\right\} - \\ &- b_{np}^{TE}\mathbf{h}_{1,np}^{TE}\exp\left\{-j\beta_{1,np}^{TE}z\right\}]\end{aligned} \tag{41}$$

where $b_{np}^{TM,TE}$ are unknown coeficients to be determined.

Finally, the transversal field in region 2 is expressed as a superposition of both $+z$ and $-z$ propagating modes, namely:

$$
\begin{aligned}
\mathbf{E}_2^t &= \sum_{m=0}^{\infty}\sum_{q=1}^{\infty}[c_{mq}^{TM}\mathbf{e}_{2,mq}^{TM}\exp\left\{j\beta_{2,mq}^{TM}z\right\} + \\
&+ c_{mq}^{TE}\mathbf{e}_{2,mq}^{TE}\exp\left\{j\beta_{2,mq}^{TE}z\right\}] + \\
&+ \sum_{m=0}^{\infty}\sum_{q=1}^{\infty}[d_{mq}^{TM}\mathbf{e}_{2,mq}^{TM}\exp\left\{-j\beta_{2,mq}^{TM}z\right\} + \\
&+ d_{mq}^{TE}\mathbf{e}_{2,mq}^{TE}\exp\left\{-j\beta_{2,mq}^{TE}z\right\}] + \\
&+ c_{00}^{TEM}\mathbf{e}_2^{TEM}\exp\{jkz\} + d_{00}^{TEM}\mathbf{e}_2^{TEM}\exp\{-jkz\} \qquad (42)
\end{aligned}
$$

$$
\begin{aligned}
\mathbf{H}_2^t &= \sum_{m=0}^{\infty}\sum_{q=1}^{\infty}[c_{mq}^{TM}\mathbf{h}_{2,mq}^{TM}\exp\left\{j\beta_{2,mq}^{TM}z\right\} + \\
&+ c_{mq}^{TE}\mathbf{h}_{2,mq}^{TE}\exp\left\{j\beta_{2,mq}^{TE}z\right\}] + \\
&+ \sum_{m=0}^{\infty}\sum_{q=1}^{\infty}[-d_{mq}^{TM}\mathbf{h}_{2,mq}^{TM}\exp\left\{-j\beta_{2,mq}^{TM}z\right\} - d_{mq}^{TE}\mathbf{h}_{2,mq}^{TE}\exp\left\{-j\beta_{2,mq}^{TE}z\right\}] + \\
&+ c_{00}^{TEM}\mathbf{h}_2^{TEM}\exp\{jkz\} - d_{00}^{TEM}\mathbf{h}_2^{TEM}\exp\{-jkz\} \qquad (43)
\end{aligned}
$$

Let us locate the origin of the coordinate system at the interface between the two regions. Our goal is to determine $b_{np}^{TM,TE}, c_{mq}^{TM,TE}, d_{mq}^{TM,TE}$ by enforcing the tangential field continuity condition at the interface between the two regions and the

$$
\mathbf{E}_2^t(z=-l_2) = \mathbf{0} \qquad (44)
$$

condition at the inlet termination. From eq. (44) we get

$$d_{mq}^{TM} = -c_{mq}^{TM} \exp\left\{-2j\beta_{2,mq}^{TM} l_2\right\} \quad (45)$$

$$d_{mq}^{TE} = -c_{mq}^{TE} \exp\left\{-2j\beta_{2,mq}^{TE} l_2\right\} \quad (46)$$

$$d_{00}^{TEM} = -c_{00}^{TEM} \exp\left\{-2jkl_2\right\} \quad (47)$$

The boundary conditions at the interface are

$$\mathbf{E}_1^{ti}(z=0) + \mathbf{E}_1^{tr}(z=0) = \mathbf{E}_2^{t}(z=0) \quad (48)$$

$$\mathbf{H}_1^{ti}(z=0) + \mathbf{H}_1^{tr}(z=0) = \mathbf{H}_2^{t}(z=0) \quad (49)$$

$$\forall\rho \in [a,b], \forall\phi \in [0,2\pi]$$

Also, the tangential field in region 1 for $0 \leq \rho < a$ has to be identically equal to zero due to the conducting surface defined by $0 \leq \rho < a, z = 0$.

By enforcing (38)-(43) and (45),(46), (47), we obtain the following equations

$$\sum_{n=0}^{\infty}\sum_{p=1}^{\infty}\left[\left(a_{np}^{TM} + b_{np}^{TM}\right)\mathbf{e}_{1,np}^{TM} + \left(a_{np}^{TE} + b_{np}^{TE}\right)\mathbf{e}_{1,np}^{TE}\right] =$$

$$= \sum_{n=0}^{\infty}\sum_{p=1}^{\infty}\left[c_{np}^{TM} f_{np}^{TM} \mathbf{e}_{2,np}^{TM} + c_{np}^{TE} f_{np}^{TE} \mathbf{e}_{2,np}^{TE}\right] +$$

$$+ \; c_{00}^{TEM} f_{00}^{TEM} \mathbf{e}_2^{TEM} \tag{50}$$

and

$$\sum_{n=0}^{\infty}\sum_{p=1}^{\infty}\left[\left(a_{np}^{TM} - b_{np}^{TM}\right)\mathbf{h}_{1,np}^{TM} + \left(a_{np}^{TE} - b_{np}^{TE}\right)\mathbf{h}_{1,np}^{TE}\right] =$$

$$= \sum_{n=0}^{\infty}\sum_{p=1}^{\infty}\left[c_{np}^{TM} g_{np}^{TM} \mathbf{h}_{2,np}^{TM} + c_{np}^{TE} g_{np}^{TE} \mathbf{h}_{2,np}^{TE}\right] +$$

$$+ \; c_{00}^{TEM} g_{00}^{TEM} \mathbf{h}_2^{TEM} \tag{51}$$

where, by definition

$$f_{np}^{TM} \equiv 1 - \exp\left\{-2j\beta_{2,np}^{TM} l_2\right\} \tag{52}$$

$$g_{np}^{TM} \equiv 1 + \exp\left\{-2j\beta_{2,np}^{TM} l_2\right\} \tag{53}$$

$$f_{np}^{TE} \equiv 1 - \exp\left\{-2j\beta_{2,np}^{TE} l_2\right\} \tag{54}$$

$$g_{np}^{TE} \equiv 1 + \exp\left\{-2j\beta_{2,np}^{TE} l_2\right\} \tag{55}$$

$$f_{00}^{TEM} \equiv 1 - \exp\left\{-2jkl_2\right\} \tag{56}$$

$$g_{00}^{TEM} \equiv 1 + \exp\left\{-2jkl_2\right\} \tag{57}$$

Next, on applying mode orthogonality, $c_{ij}^{TM,TE,TEM}$ coefficients can be eliminated from eq. (50) and (51). The elimination has to be done in such a

way that the condition $\mathbf{E}_1^t(z=0), 0 \leq \rho < a, z = 0$ is taken into account. Specifically, on taking the dot product of (50) with $\mathbf{e}_{1,mq}^{TM}$ and integrating over the *whole* interface, we obtain

$$\begin{aligned} & \left(a_{mq}^{TM} + b_{mq}^{TM}\right) U_{mq}^{TM} = \\ = & \sum_{n=0}^{\infty} \sum_{p=1}^{\infty} \left[c_{np}^{TM} f_{np}^{TM} P_{np,mq}^{TM} + c_{np}^{TE} f_{np}^{TE} P_{np,mq}^{TE}\right] + \\ + & c_{00}^{TEM} f_{00}^{TEM} P_{00,mq}^{TEM} \end{aligned} \tag{58}$$

where, by definition

$$P_{mq,np}^{TM} \equiv \int_a^b \int_0^{2\pi} \mathbf{e}_{2,mq}^{TM} \cdot \mathbf{e}_{1,np}^{TM} \rho d\rho d\phi \tag{59}$$

$$P_{mq,np}^{TE} \equiv \int_a^b \int_0^{2\pi} \mathbf{e}_{2,mq}^{TE} \cdot \mathbf{e}_{1,np}^{TM} \rho d\rho d\phi \tag{60}$$

$$P_{00,np}^{TEM} \equiv \int_a^b \int_0^{2\pi} \mathbf{e}_{2}^{TEM} \cdot \mathbf{e}_{1,np}^{TM} \rho d\rho d\phi \tag{61}$$

$$U_{mq}^{TM} \equiv \int_0^b \int_0^{2\pi} \mathbf{e}_{1,mq}^{TM} \cdot \mathbf{e}_{1,mq}^{TM} \rho d\rho d\phi \tag{62}$$

Similarly, on taking the dot product of (50) with $\mathbf{e}_{1,mq}^{TE}$ and integrating over the whole interface, we obtain

$$\left(a_{mq}^{TE} + b_{mq}^{TE}\right) U_{mq}^{TE} =$$

$$= \sum_{n=0}^{\infty}\sum_{p=1}^{\infty}\left[c_{np}^{TM} f_{np}^{TM} Q_{np,mq}^{TM} + c_{np}^{TE} f_{np}^{TE} Q_{np,mq}^{TE}\right] +$$

$$+ \quad c_{00}^{TEM} f_{00}^{TEM} Q_{00,mq}^{TEM} \tag{63}$$

where, by definition

$$Q_{mq,np}^{TM} \equiv \int_a^b \int_0^{2\pi} \mathbf{e}_{2,mq}^{TM} \cdot \mathbf{e}_{1,np}^{TE} \rho d\rho d\phi \tag{64}$$

$$Q_{mq,np}^{TE} \equiv \int_a^b \int_0^{2\pi} \mathbf{e}_{2,mq}^{TE} \cdot \mathbf{e}_{1,np}^{TE} \rho d\rho d\phi \tag{65}$$

$$Q_{00,np}^{TEM} \equiv \int_a^b \int_0^{2\pi} \mathbf{e}_{2}^{TEM} \cdot \mathbf{e}_{1,np}^{TE} \rho d\rho d\phi \tag{66}$$

$$U_{mq}^{TE} \equiv \int_0^b \int_0^{2\pi} \mathbf{e}_{1,mq}^{TE} \cdot \mathbf{e}_{1,mq}^{TE} \rho d\rho d\phi \tag{67}$$

Next, on taking the dot product of (51) with $\mathbf{h}_{2,mq}^{TM}$ and integrating over the *common* portion of the interface, we obtain

$$V_{mq}^{TM} g_{mq}^{TM} c_{mq}^{TM} =$$

$$= \sum_{n=0}^{\infty}\sum_{p=1}^{\infty}\left[\left(a_{np}^{TM} - b_{np}^{TM}\right) R_{mq,np}^{TM} + \left(a_{np}^{TE} - b_{np}^{TE}\right) S_{mq,np}^{TM}\right] \tag{68}$$

where, by definition

$$R_{mq,np}^{TM} \equiv \int_a^b \int_0^{2\pi} \mathbf{h}_{2,mq}^{TM} \cdot \mathbf{h}_{1,np}^{TM} \rho d\rho d\phi \tag{69}$$

$$S^{TM}_{mq,np} \equiv \int_a^b \int_0^{2\pi} \mathbf{h}^{TM}_{2,mq} \cdot \mathbf{h}^{TE}_{1,np} \rho d\rho d\phi \tag{70}$$

$$V^{TM}_{mq} \equiv \int_a^b \int_0^{2\pi} \mathbf{h}^{TM}_{2,mq} \cdot \mathbf{h}^{TM}_{2,mq} \rho d\rho d\phi \tag{71}$$

Similarly, on taking the dot product of (51) with $\mathbf{h}^{TE}_{2,mq}$ and integrating over the common portion of the interface, we obtain

$$V^{TE}_{mq} g^{TE}_{mq} c^{TE}_{mq} =$$

$$= \sum_{n=0}^{\infty} \sum_{p=1}^{\infty} \left[\left(a^{TM}_{np} - b^{TM}_{np} \right) R^{TE}_{mq,np} + \left(a^{TE}_{np} - b^{TE}_{np} \right) S^{TE}_{mq,np} \right] \tag{72}$$

where, by definition

$$R^{TE}_{mq,np} \equiv \int_a^b \int_0^{2\pi} \mathbf{h}^{TE}_{2,mq} \cdot \mathbf{h}^{TM}_{1,np} \rho d\rho d\phi \tag{73}$$

$$S^{TE}_{mq,np} \equiv \int_a^b \int_0^{2\pi} \mathbf{h}^{TE}_{2,mq} \cdot \mathbf{h}^{TE}_{1,np} \rho d\rho d\phi \tag{74}$$

$$V^{TE}_{mq} \equiv \int_a^b \int_0^{2\pi} \mathbf{h}^{TE}_{2,mq} \cdot \mathbf{h}^{TE}_{2,mq} \rho d\rho d\phi \tag{75}$$

Finally, on taking the dot product of (51) with $\mathbf{h}^{TEM}_{2}$ and integrating over the common portion of the interface, we obtain

$$V^{TEM}_{00} g^{TEM}_{00} c^{TEM}_{00} =$$

$$= \sum_{n=0}^{\infty}\sum_{p=1}^{\infty}\left[\left(a_{np}^{TM}-b_{np}^{TM}\right)R_{00,np}^{TEM}+\left(a_{np}^{TE}-b_{np}^{TE}\right)S_{00,np}^{TEM}\right] \tag{76}$$

where, by definition

$$R_{00,np}^{TEM} \equiv \int_a^b\int_0^{2\pi}\mathbf{h}_2^{TEM}\cdot\mathbf{h}_{1,np}^{TM}\rho d\rho d\phi \tag{77}$$

$$S_{00,np}^{TEM} \equiv \int_a^b\int_0^{2\pi}\mathbf{h}_2^{TEM}\cdot\mathbf{h}_{1,np}^{TE}\rho d\rho d\phi \tag{78}$$

$$V_{00}^{TEM} \equiv \int_a^b\int_0^{2\pi}\mathbf{h}_2^{TEM}\cdot\mathbf{h}_2^{TEM}\rho d\rho d\phi \tag{79}$$

The elimination of the $c_{np}^{TM,TE,TEM}$ coefficients from eq. (58), (63), (68), (72), (76) is easier if we write the latter equations in matrix form. Let i be an integer that combines m and q and let j be an integer that combines n and p. Let M_k be the number of TM modes in region k and N_k the number of TE modes in region k ($k=1,2$). Evidently, $M_k, N_k \to \infty$. Let

$$\{\mathbf{a}\} \equiv \left[a_1^{TM},...,a_{M_1}^{TM},a_1^{TE},...,a_{N_1}^{TE}\right]^T \tag{80}$$

$$\{\mathbf{b}\} \equiv \left[b_1^{TM},...,b_{M_1}^{TM},b_1^{TE},...,b_{N_1}^{TE}\right]^T \tag{81}$$

$$\{\mathbf{c}\} \equiv \left[c_1^{TM},...,c_{M_2}^{TM},c_1^{TE},...,c_{N_2}^{TE},c_0^{TEM}\right]^T \tag{82}$$

$$[\mathbf{V}] \equiv \mathbf{diag}\left[V_1^{TM},...,V_{M_2}^{TM},V_1^{TE},...,V_{N_2}^{TE},V_0^{TEM}\right] \tag{83}$$

$$[\mathbf{U}] \equiv \mathbf{diag}\left[U_1^{TM},...,U_{M_1}^{TM},U_1^{TE},...,U_{N_1}^{TE}\right] \tag{84}$$

$$[\mathbf{F}] \equiv \mathbf{diag}\left[f_1^{TM},...,f_{M_2}^{TM},f_1^{TE},...,f_{N_2}^{TE},f_0^{TEM}\right] \tag{85}$$

$$[\mathbf{G}] \equiv \mathbf{diag}\left[g_1^{TM},...,g_{M_2}^{TM},g_1^{TE},...,g_{N_2}^{TE},g_0^{TEM}\right] \tag{86}$$

Moreover, let

$$[\mathbf{K}] \equiv \begin{bmatrix} P_{1,1}^{TM} & ... & P_{1,M_1}^{TM} & Q_{1,1}^{TM} & ... & Q_{1,N_1}^{TM} \\ P_{2,1}^{TM} & ... & P_{2,M_1}^{TM} & Q_{2,1}^{TM} & ... & Q_{2,N_1}^{TM} \\ ... & ... & ... & ... & ... & ... \\ P_{M_2,1}^{TM} & ... & P_{M_2,M_1}^{TM} & Q_{M_2,1}^{TM} & ... & Q_{M_2,N_1}^{TM} \\ P_{1,1}^{TE} & ... & P_{1,M_1}^{TE} & Q_{1,1}^{TE} & ... & Q_{1,N_1}^{TE} \\ P_{2,1}^{TE} & ... & P_{2,M_1}^{TE} & Q_{2,1}^{TE} & ... & Q_{2,N_1}^{TE} \\ ... & ... & ... & ... & ... & ... \\ P_{N_2,1}^{TE} & ... & P_{N_2,M_1}^{TE} & Q_{N_2,1}^{TE} & ... & Q_{N_2,N_1}^{TE} \\ P_{0,1}^{TEM} & ... & P_{0,M_1}^{TEM} & Q_{0,1}^{TEM} & ... & Q_{0,N_1}^{TEM} \end{bmatrix} \tag{87}$$

and

$$[\mathbf{L}] \equiv \begin{bmatrix} R_{1,1}^{TM} & ... & R_{1,M_1}^{TM} & S_{1,1}^{TM} & ... & S_{1,N_1}^{TM} \\ R_{2,1}^{TM} & ... & R_{2,M_1}^{TM} & S_{2,1}^{TM} & ... & S_{2,N_1}^{TM} \\ ... & ... & ... & ... & ... & ... \\ R_{M_2,1}^{TM} & ... & R_{M_2,M_1}^{TM} & S_{M_2,1}^{TM} & ... & S_{M_2,N_1}^{TM} \\ R_{1,1}^{TE} & ... & R_{1,M_1}^{TE} & S_{1,1}^{TE} & ... & S_{1,N_1}^{TE} \\ R_{2,1}^{TE} & ... & R_{2,M_1}^{TE} & S_{2,1}^{TE} & ... & S_{2,N_1}^{TE} \\ ... & ... & ... & ... & ... & ... \\ R_{N_2,1}^{TE} & ... & R_{N_2,M_1}^{TE} & S_{N_2,1}^{TE} & ... & S_{N_2,N_1}^{TE} \\ R_{0,1}^{TEM} & ... & R_{0,M_1}^{TEM} & S_{0,1}^{TEM} & ... & S_{0,N_1}^{TEM} \end{bmatrix} \tag{88}$$

Under the latter definitions, eq. (58), (63), (68), (72), (76) can be written in the following compact form:

$$[\mathbf{U}](\{\mathbf{a}\}+\{\mathbf{b}\}) = [\mathbf{K}]^T[\mathbf{F}]\{\mathbf{c}\} \tag{89}$$

$$[\mathbf{L}](\{\mathbf{a}\} - \{\mathbf{b}\}) = [\mathbf{G}][\mathbf{V}]\{\mathbf{c}\} \tag{90}$$

It is straightforward to show that the two latter matrix equations yield

$$\{\mathbf{b}\} = ([\mathbf{W}] + [\mathbf{I}])^{-1}([\mathbf{W}] - [\mathbf{I}])\{\mathbf{a}\} \tag{91}$$

where

$$[\mathbf{W}] = [\mathbf{U}]^{-1}[\mathbf{K}]^{T}[\mathbf{F}][\mathbf{V}]^{-1}[\mathbf{G}]^{-1}[\mathbf{L}] \tag{92}$$

and [**I**] is the unitary matrix. Closed form expressions for all the involved coefficients are found in Appendix I.

It is evident from (91) that an infinite matrix has to be inverted, therefore extreme care has to be taken, since taking the limit of the results of conventional solution techniques is not straightforward. Mittra and Lee [2] discuss the difficulties encountered in such a process. For computational purposes only a finite number of modes in each region can be used, i.e. all the propagating ones and a finite number of the most significant evanescent ones.

As we have already mentioned, the Mode Matching Technique is useful and efficient only for small structures, where the number of propagating modes is reasonably low. For large structures, the matrix that has to be

inverted becomes very big. Apart from the fact that the inversion is very time-consuming, the problem may become ill-conditioned. The condition number of the matrix to be inverted may exceed 10^{10}, making the results unreliable.

3 Numerical Results for a Circular Inlet Terminated by a Cylindrical Hub

Figures 4-7 show some numerical results for the geometry of Fig. 3. For all cases, in the Mode Matching method, 420 modes were used for each region, i.e. the order of the cylindrical functions ranged from $n = 0$ to $n = 14$ and 7 modes for each n were taken into account (i.e. we have $15 \cdot 7 = 105$ TM modes, plus 105 TE modes, multiplied by 2 for even and odd angular behavior. For the second region, the TEM mode substituted one of the less important evanescent TM modes). The Mode Matching results are being compared to those of the Hybrid Modal Technique [10]. In the latter technique, the termination is modeled by the Moment Method. The agreement is, in general, very good, except in the horizontal polarization case for the small geometry (figure 7). According to [10] the results of the Hybrid Modal Technique for this case may not be perfect because some approximations have been

introduced which are associated with the physical break-up of the duct from the termination. The error gets worse for wide angles and smaller cylinders. On the contrary, the Mode Matching technique does not suffer from such a limitation.

It is worth mentioning that the results converge rather slowly, and that a smaller number of modes may not yield correct values for the RCS. On the other hand, a larger number of modes requires the inversion of a larger matrix with a larger condition number, resulting to inaccurate values, too. Finally, one should bear in mind the fact that the results are not valid for the neighborhood of grazing incidence, since the formulas given in Appendix IV were derived provided that the plane wave incident takes place at an angle not too far away from the cylinder axis.

Figures 8 and 9 depict the amplitudes of the elements of the generalized scattering matrix corresponding to the above geometries. It is evident that there is coupling only among modes of the same order (i.e. order of the cylindrical function). This fact can be shown analytically. It can also be shown analytically that TM and TE modes do not couple to TM and TE modes (respectively) of different angular variation, e.g. a TM mode of $\cos n\phi$ variation does not couple to a TM of $\sin n\phi$ variation. Intercoupling among

TM and TE modes, though, occurs only if the two modes do have different angular variation. Moreover, the coupling between any two given modes remains the same if the angular variations of both modes are switched. Finally, all modes couple significantly only to their closest neighbors, resulting to almost banded scattering matrices. Large off-diagonal elements (whenever they occur) correspond to evanescent modes.

4 Mode Matching Formulation for a Hollow Cylinder Terminated by a Periodic Array of Grooves

In this section we will apply the same Mode Matching technique to the more complicated geometry of a hollow cylinder terminated by a cylindrical array of grooves. The geometry is depicted in Fig. 8. Evidently, the modes in region 1 are identical to those of the previous geometry. The modes occuring in each one of the grooves of this termination are analytically evaluated in Appendix II. Let us assume that the array consists of J grooves, which are essentially cylindrical (pie-shell) sectors terminated by a short. Then, given that the rightmost edge of the first groove makes an angle ϕ_1 with the x-axis, the rightmost edge of the κ^{th} groove will form the angle

$$\phi_\kappa = \phi_1 + (\kappa - 1)\frac{2\pi}{J} \tag{93}$$

with the x-axis, where ϕ_w is the angular extent of each groove. The fields in the κ^{th} groove can be explicitly written as follows (see eq. (23), (24) and Appendix II):

Region 2 (κ^{th} groove).

$$\begin{aligned}
\mathbf{e}^{TM}_{2,\kappa,mq} &= \gamma^{TM}_{2,mq}\left[Y_\nu\left(\gamma^{TM}_{2,mq}a\right)J'_\nu\left(\gamma^{TM}_{2,mq}\rho\right) - J_\nu\left(\gamma^{TM}_{2,mq}a\right)Y'_\nu\left(\gamma^{TM}_{2,mq}\rho\right)\right]\cdot \\
&\cdot\ N^{TM}_{2,mq}\frac{\beta^{TM}_{2,mq}}{\omega\epsilon}\sin\left[\nu\left(\phi-\phi_\kappa\right)\right]\mathbf{u}_\rho + \\
&+\ \frac{\nu}{\rho}\left[Y_\nu\left(\gamma^{TM}_{2,mq}a\right)J_\nu\left(\gamma^{TM}_{2,mq}\rho\right) - J_\nu\left(\gamma^{TM}_{2,mq}a\right)Y_\nu\left(\gamma^{TM}_{2,mq}\rho\right)\right]\cdot \\
&\cdot\ N^{TM}_{2,mq}\frac{\beta^{TM}_{2,mq}}{\omega\epsilon}\cos\left[\nu\left(\phi-\phi_\kappa\right)\right]\mathbf{u}_\phi
\end{aligned} \tag{94}$$

$$\begin{aligned}
\mathbf{h}^{TM}_{2,\kappa,mq} &= \frac{\nu}{\rho}\left[Y_\nu\left(\gamma^{TM}_{2,mq}a\right)J_\nu\left(\gamma^{TM}_{2,mq}\rho\right) - J_\nu\left(\gamma^{TM}_{2,mq}a\right)Y_\nu\left(\gamma^{TM}_{2,mq}\rho\right)\right]\cdot \\
&\cdot\ N^{TM}_{2,mq}\cos\left[\nu\left(\phi-\phi_\kappa\right)\right]\mathbf{u}_\rho - \\
&-\ \gamma^{TM}_{2,mq}\left[Y_\nu\left(\gamma^{TM}_{2,mq}a\right)J'_\nu\left(\gamma^{TM}_{2,mq}\rho\right) - J_\nu\left(\gamma^{TM}_{2,mq}a\right)Y'_\nu\left(\gamma^{TM}_{2,mq}\rho\right)\right]\cdot \\
&\cdot\ N^{TM}_{2,mq}\sin\left[\nu\left(\phi-\phi_\kappa\right)\right]\mathbf{u}_\phi
\end{aligned} \tag{95}$$

$$\begin{aligned}
\mathbf{e}_{2,\kappa,mq}^{TE} &= \frac{\nu}{\rho}\left[Y_\nu'\left(\gamma_{2,mq}^{TE}a\right)J_\nu\left(\gamma_{2,mq}^{TE}\rho\right) - J_\nu'\left(\gamma_{2,mq}^{TE}a\right)Y_\nu\left(\gamma_{2,mq}^{TE}\rho\right)\right]\cdot \\
&\cdot\ N_{2,mq}^{TE}\sin\left[\nu\left(\phi-\phi_\kappa\right)\right]\mathbf{u}_\rho + \\
&+\ \gamma_{2,mq}^{TE}\left[Y_\nu'\left(\gamma_{2,mq}^{TE}a\right)J_\nu'\left(\gamma_{2,mq}^{TE}\rho\right) - J_\nu'\left(\gamma_{2,mq}^{TE}a\right)Y_\nu'\left(\gamma_{2,mq}^{TE}\rho\right)\right]\cdot \\
&\cdot\ N_{2,mq}^{TE}\cos\left[\nu\left(\phi-\phi_\kappa\right)\right]\mathbf{u}_\phi \qquad (96)
\end{aligned}$$

$$\begin{aligned}
\mathbf{h}_{2,\kappa,mq}^{TE} &= \gamma_{2,mq}^{TE}\left[Y_\nu'\left(\gamma_{2,mq}^{TE}a\right)J_\nu'\left(\gamma_{2,mq}^{TE}\rho\right) - J_\nu'\left(\gamma_{2,mq}^{TE}a\right)Y_\nu'\left(\gamma_{2,mq}^{TE}\rho\right)\right]\cdot \\
&\cdot\ N_{2,mq}^{TE}\frac{\beta_{2,mq}^{TE}}{\omega\mu}\cos\left[\nu\left(\phi-\phi_\kappa\right)\right]\mathbf{u}_\rho - \\
&-\ \frac{\nu}{\rho}\left[Y_\nu'\left(\gamma_{2,mq}^{TE}a\right)J_\nu\left(\gamma_{2,mq}^{TE}\rho\right) - J_\nu'\left(\gamma_{2,mq}^{TE}a\right)Y_\nu\left(\gamma_{2,mq}^{TE}\rho\right)\right]\cdot \\
&\cdot\ N_{2,mq}^{TE}\frac{\beta_{2,mq}^{TE}}{\omega\mu}\sin\left[\nu\left(\phi-\phi_\kappa\right)\right]\mathbf{u}_\phi \qquad (97)
\end{aligned}$$

where

$$\nu = \frac{m\pi}{\phi_w}, \qquad m \in \mathbf{N}_0 \qquad (98)$$

$$N_{2,mq}^{TM} \equiv -\frac{\omega\epsilon}{\beta_{2,np}^{TM}}\frac{1}{2}\sqrt{\frac{\phi_w\left(3-\epsilon_m\right)}{2}}\left[\frac{J_m^2\left(\gamma_{2,mq}^{TM}a\right)}{J_m^2\left(\gamma_{2,mq}^{TM}b\right)} - 1\right]^{-\frac{1}{2}} \qquad (99)$$

$$\begin{aligned}
N_{2,mq}^{TE} &\equiv \frac{1}{2}\sqrt{\frac{\phi_w\left(3-\epsilon_m\right)}{2}}\left\{\left[\frac{J_m'\left(\gamma_{2,mq}^{TE}a\right)}{J_m'\left(\gamma_{2,mq}^{TE}b\right)}\right]^2\left[1-\left(\frac{m}{\gamma_{2,mq}^{TE}b}\right)^2\right] - \right. \\
&-\ \left.\left[1-\left(\frac{m}{\gamma_{2,mq}^{TE}a}\right)^2\right]\right\}^{-\frac{1}{2}} \qquad (100)
\end{aligned}$$

and $\gamma_{2,mq}^{TM,TE}, \beta_{2,mq}^{TM,TE}$ are defined in Appendix II. Note the evident absence of TEM modes (since there is only one conductor).

The boundary conditions at the interface are:

$$\mathbf{E}_1^{ti}(z=0) + \mathbf{E}_1^{tr}(z=0) = \mathbf{E}_2^{t}(z=0) \tag{101}$$

$$\mathbf{H}_1^{ti}(z=0) + \mathbf{H}_1^{tr}(z=0) = \mathbf{H}_2^{t}(z=0) \tag{102}$$

$$\forall \rho \in [a,b], \forall \phi \in [\phi_\kappa, \phi_\kappa + \phi_w], \forall \kappa \in \{1,...,J\}$$

and

$$\mathbf{E}_1^{ti}(z=0) + \mathbf{E}_1^{tr}(z=0) = \mathbf{0} \qquad \text{elsewhere} \tag{103}$$

Following the same procedure used for the previous geometry, (101)-(103) result in the following system of equations:

$$\left(a_{mq}^{TM} + b_{mq}^{TM}\right) U_{mq}^{TM} =$$

$$= \sum_{\kappa=1}^{J} \sum_{n=0}^{\infty} \sum_{p=1}^{\infty} \left[c_{\kappa,np}^{TM} f_{np}^{TM} P_{\kappa,np,mq}^{TM} + c_{\kappa,np}^{TE} f_{np}^{TE} P_{\kappa,np,mq}^{TE} \right] \tag{104}$$

$$\left(a_{mq}^{TE} + b_{mq}^{TE}\right) U_{mq}^{TE} =$$

$$= \sum_{\kappa=1}^{J} \sum_{n=0}^{\infty} \sum_{p=1}^{\infty} \left[c_{\kappa,np}^{TM} f_{np}^{TM} Q_{\kappa,np,mq}^{TM} + c_{\kappa,np}^{TE} f_{np}^{TE} Q_{\kappa,np,mq}^{TE} \right] \tag{105}$$

and

$$V^{TM}_{\kappa,mq} g^{TM}_{mq} c^{TM}_{\kappa,mq} =$$

$$= \sum_{n=0}^{\infty} \sum_{p=1}^{\infty} \left[\left(a^{TM}_{np} - b^{TM}_{np} \right) R^{TM}_{\kappa,mq,np} + \left(a^{TE}_{np} - b^{TE}_{np} \right) S^{TM}_{\kappa,mq,np} \right] \quad (106)$$

$$V^{TE}_{\kappa,mq} g^{TE}_{mq} c^{TE}_{\kappa,mq} =$$

$$= \sum_{n=0}^{\infty} \sum_{p=1}^{\infty} \left[\left(a^{TM}_{np} - b^{TM}_{np} \right) R^{TE}_{\kappa,mq,np} + \left(a^{TE}_{np} - b^{TE}_{np} \right) S^{TE}_{\kappa,mq,np} \right] \quad (107)$$

$$\forall \kappa \in \{1, ..., J\}$$

where, by definition

$$P^{TM}_{\kappa,mq,np} \equiv \int_a^b \int_{\phi_\kappa}^{\phi_\kappa + \phi_w} \mathbf{e}^{TM}_{2,\kappa,mq} \cdot \mathbf{e}^{TM}_{1,np} \rho d\rho d\phi \quad (108)$$

$$P^{TE}_{\kappa,mq,np} \equiv \int_a^b \int_{\phi_\kappa}^{\phi_\kappa + \phi_w} \mathbf{e}^{TE}_{2,\kappa,mq} \cdot \mathbf{e}^{TM}_{1,np} \rho d\rho d\phi \quad (109)$$

$$U^{TM}_{mq} \equiv \int_0^b \int_0^{2\pi} \mathbf{e}^{TM}_{1,mq} \cdot \mathbf{e}^{TM}_{1,mq} \rho d\rho d\phi \quad (110)$$

$$Q^{TM}_{\kappa,mq,np} \equiv \int_a^b \int_{\phi_\kappa}^{\phi_\kappa + \phi_w} \mathbf{e}^{TM}_{2,\kappa,mq} \cdot \mathbf{e}^{TE}_{1,np} \rho d\rho d\phi \quad (111)$$

$$Q^{TE}_{\kappa,mq,np} \equiv \int_a^b \int_{\phi_\kappa}^{\phi_\kappa + \phi_w} \mathbf{e}^{TE}_{2,\kappa,mq} \cdot \mathbf{e}^{TE}_{1,np} \rho d\rho d\phi \quad (112)$$

$$U^{TE}_{mq} \equiv \int_0^b \int_0^{2\pi} \mathbf{e}^{TE}_{1,mq} \cdot \mathbf{e}^{TE}_{1,mq} \rho d\rho d\phi \quad (113)$$

$$R^{TM}_{\kappa,mq,np} \equiv \int_a^b \int_{\phi_\kappa}^{\phi_\kappa + \phi_w} \mathbf{h}^{TM}_{2,\kappa,mq} \cdot \mathbf{h}^{TM}_{1,np} \rho d\rho d\phi \quad (114)$$

$$S^{TM}_{\kappa,mq,np} \equiv \int_a^b \int_{\phi_\kappa}^{\phi_\kappa + \phi_w} \mathbf{h}^{TM}_{2,\kappa,mq} \cdot \mathbf{h}^{TE}_{1,np} \rho d\rho d\phi \quad (115)$$

$$V^{TM}_{\kappa,mq} \equiv \int_a^b \int_{\phi_\kappa}^{\phi_\kappa + \phi_w} \mathbf{h}^{TM}_{2,\kappa,mq} \cdot \mathbf{h}^{TM}_{2,\kappa,mq} \rho d\rho d\phi \quad (116)$$

$$R^{TE}_{\kappa,mq,np} \equiv \int_a^b \int_{\phi_\kappa}^{\varphi_\kappa+\phi_w} \mathbf{h}^{TE}_{2,\kappa,mq} \cdot \mathbf{h}^{TM}_{1,np} \rho d\rho d\phi \tag{117}$$

$$S^{TE}_{\kappa,mq,np} \equiv \int_a^b \int_{\phi_\kappa}^{\phi_\kappa+\phi_w} \mathbf{h}^{TE}_{2,\kappa,mq} \cdot \mathbf{h}^{TE}_{1,np} \rho d\rho d\phi \tag{118}$$

$$V^{TE}_{\kappa,mq} \equiv \int_a^b \int_{\phi_\kappa}^{\phi_\kappa+\phi_w} \mathbf{h}^{TE}_{2,\kappa,mq} \cdot \mathbf{h}^{TE}_{2,\kappa,mq} \rho d\rho d\phi \tag{119}$$

and $f^{TM,TE}_{np}, g^{TM,TE}_{np}$ are defined in the same way as in (52)-(55), identically for each of the J grooves. Note that the system of equations and the definition of the coefficients are formally almost identical to the corresponding ones of the previous geometry, the only difference being the presence of an extra index, κ, which identifies the κ^{th} of the J grooves. For numerical implementation let us truncate the above infinite series to M_1 TM modes in region 1, N_1 TE modes in region 1, M_2 TM modes in any given groove of region 2 and N_2 TE modes in any given groove in region 2. Similarly to the previous case, it is convenient to define the following matrices (after transforming the double indices to single ones):

$$\{\mathbf{a}\} \equiv \left[a^{TM}_1, ..., a^{TM}_{M_1}, a^{TE}_1, ..., a^{TE}_{N_1}\right]^T \tag{120}$$

$$\{\mathbf{b}\} \equiv \left[b^{TM}_1, ..., b^{TM}_{M_1}, b^{TE}_1, ..., b^{TE}_{N_1}\right]^T \tag{121}$$

$$\{\mathbf{c}_\kappa\} \equiv \left[c^{TM}_{\kappa,1}, ..., c^{TM}_{\kappa,M_2}, c^{TE}_{\kappa,1}, ..., c^{TE}_{\kappa,N_2}\right]^T \tag{122}$$

$$[\mathbf{V}_\kappa] \equiv \mathbf{diag}\left[V_{\kappa,1}^{TM},...,V_{\kappa,M_2}^{TM},V_{\kappa,1}^{TE},....,V_{\kappa,N_2}^{TE}\right] \tag{123}$$

$$[\mathbf{U}] \equiv \mathbf{diag}\left[U_1^{TM},...,U_{M_1}^{TM},U_1^{TE},...,U_{N_1}^{TE}\right] \tag{124}$$

$$[\mathbf{F}_\kappa] \equiv \mathbf{diag}\left[f_1^{TM},...,f_{M_2}^{TM},f_1^{TE},...,f_{N_2}^{TE}\right] \tag{125}$$

$$[\mathbf{G}_\kappa] \equiv \mathbf{diag}\left[g_1^{TM},...,g_{M_2}^{TM},g_1^{TE},...,g_{N_2}^{TE}\right] \tag{126}$$

(Note that, because the f and g parameters are identical for all the grooves, $[\mathbf{F}_\kappa]$ and $[\mathbf{G}_\kappa]$ do not vary with κ).

Also, let

$$[\mathbf{K}_\kappa] \equiv \begin{bmatrix} P_{\kappa,1,1}^{TM} & \cdots & P_{\kappa,1,M_1}^{TM} & Q_{\kappa,1,1}^{TM} & \cdots & Q_{\kappa,1,N_1}^{TM} \\ P_{\kappa,2,1}^{TM} & \cdots & P_{\kappa,2,M_1}^{TM} & Q_{\kappa,2,1}^{TM} & \cdots & Q_{\kappa,2,N_1}^{TM} \\ \cdots & \cdots & \cdots & \cdots & \cdots & \cdots \\ P_{\kappa,M_2,1}^{TM} & \cdots & P_{\kappa,M_2,M_1}^{TM} & Q_{\kappa,M_2,1}^{TM} & \cdots & Q_{\kappa,M_2,N_1}^{TM} \\ P_{\kappa,1,1}^{TE} & \cdots & P_{\kappa,1,M_1}^{TE} & Q_{\kappa,1,1}^{TE} & \cdots & Q_{\kappa,1,N_1}^{TE} \\ P_{\kappa,2,1}^{TE} & \cdots & P_{\kappa,2,M_1}^{TE} & Q_{\kappa,2,1}^{TE} & \cdots & Q_{\kappa,2,N_1}^{TE} \\ \cdots & \cdots & \cdots & \cdots & \cdots & \cdots \\ P_{\kappa,N_2,1}^{TE} & \cdots & P_{\kappa,N_2,M_1}^{TE} & Q_{\kappa,N_2,1}^{TE} & \cdots & Q_{\kappa,N_2,N_1}^{TE} \end{bmatrix} \tag{127}$$

$$[\mathbf{L}_\kappa] \equiv \begin{bmatrix} R_{\kappa,1,1}^{TM} & \cdots & R_{\kappa,1,M_1}^{TM} & S_{\kappa,1,1}^{TM} & \cdots & S_{\kappa,1,N_1}^{TM} \\ R_{\kappa,2,1}^{TM} & \cdots & R_{\kappa,2,M_1}^{TM} & S_{\kappa,2,1}^{TM} & \cdots & S_{\kappa,2,N_1}^{TM} \\ \cdots & \cdots & \cdots & \cdots & \cdots & \cdots \\ R_{\kappa,M_2,1}^{TM} & \cdots & R_{\kappa,M_2,M_1}^{TM} & S_{\kappa,M_2,1}^{TM} & \cdots & S_{\kappa,M_2,N_1}^{TM} \\ R_{\kappa,1,1}^{TE} & \cdots & R_{\kappa,1,M_1}^{TE} & S_{\kappa,1,1}^{TE} & \cdots & S_{\kappa,1,N_1}^{TE} \\ R_{\kappa,2,1}^{TE} & \cdots & R_{\kappa,2,M_1}^{TE} & S_{\kappa,2,1}^{TE} & \cdots & S_{\kappa,2,N_1}^{TE} \\ \cdots & \cdots & \cdots & \cdots & \cdots & \cdots \\ R_{\kappa,N_2,1}^{TE} & \cdots & R_{\kappa,N_2,M_1}^{TE} & S_{\kappa,N_2,1}^{TE} & \cdots & S_{\kappa,N_2,N_1}^{TE} \end{bmatrix} \tag{128}$$

$$\{\mathbf{c}\} \equiv \left[\{\mathbf{c}_1\}^T,\{\mathbf{c}_2\}^T,...,\{\mathbf{c}_J\}^T\right]^T \tag{129}$$

$$[\mathbf{V}] \equiv \mathbf{diag}\left[[\mathbf{V}_1], [\mathbf{V}_2], ..., [\mathbf{V}_J]\right] \tag{130}$$

$$[\mathbf{F}] \equiv \mathbf{diag}\left[[\mathbf{F}_1], [\mathbf{F}_2], ..., [\mathbf{F}_J]\right] \tag{131}$$

$$[\mathbf{G}] \equiv \mathbf{diag}\left[[\mathbf{G}_1], [\mathbf{G}_2], ..., [\mathbf{G}_J]\right] \tag{132}$$

$$[\mathbf{K}] \equiv \left[[\mathbf{K}_1]^T, [\mathbf{K}_2]^T, ..., [\mathbf{K}_J]^T\right]^T \tag{133}$$

$$[\mathbf{L}] \equiv \left[[\mathbf{L}_1]^T, [\mathbf{L}_2]^T, ..., [\mathbf{L}_J]^T\right]^T \tag{134}$$

Using these matrix definitions, the system of equations can be cast in the following compact form:

$$[\mathbf{U}](\{\mathbf{a}\} + \{\mathbf{b}\}) = [\mathbf{K}]^T [\mathbf{F}] \{\mathbf{c}\} \tag{135}$$

$$[\mathbf{L}](\{\mathbf{a}\} - \{\mathbf{b}\}) = [\mathbf{G}][\mathbf{V}]\{\mathbf{c}\} \tag{136}$$

Again, it is straightforward to show that the two latter matrix equations yield

$$\{\mathbf{b}\} = ([\mathbf{W}] + [\mathbf{I}])^{-1} ([\mathbf{W}] - [\mathbf{I}]) \{\mathbf{a}\} \tag{137}$$

where

$$[\mathbf{W}] = [\mathbf{U}]^{-1} [\mathbf{K}]^T [\mathbf{F}] [\mathbf{V}]^{-1} [\mathbf{G}]^{-1} [\mathbf{L}] \tag{138}$$

and [**I**] is the unitary matrix.

Obviously, the expressions that we derived for the unknowns {**b**} are formally identical to the corresponding expressions of the previous geometry. There are a few important differences though. The fact that the order of the cylindrical functions in the second region is, in general, non-integer and that the region of the ϕ-integration is not a full circle leads to coupling among all modes of the first and second region. In the previous case of stub termination, orthogonality among the trigonometric functions resulted in coupling only among modes of the same order, leading to banded matrices. Moreover, as opposed to the previous case, the elements of the [**K**] and [**L**] matrices cannot, in general, be evaluated in closed form, to the best of our knowledge. Numerical integration is thus necessary for the evaluation resulting in slower codes.

5 Numerical Results for a Circular Inlet Terminated by a Cylindrical Array of Grooves

Figures 12 – 15 show some numerical results for the geometry of Fig. 10. For the dimensions of Fig. 12 and 13, 800 modes were used in Region 1, i.e. the order of the cylindrical functions ranged from $n = 0$ to $n = 20$ and 10 modes

for each n were taken into account (i.e. $20 \cdot 10 = 200$ TM modes, plus 200 TE modes, multiplied by 2 for even and odd angular dependence). In Region 2 70 modes were used (i.e. $5 \cdot 7 \cdot 2$). For the dimensions of Fig. 14 and 15 we used $280 = 10 \cdot 7 \cdot 2 \cdot 2$ and $42 = 3 \cdot 7 \cdot 2$ modes respectively. Unfortunately, no reliable independent solution exists so far, hence no comparison can be made.

Figures 16 and 17 depict the amplitudes of the elements of the generalized scattering matrix. In this case there is coupling, in general, among all kinds of modes, as opposed to the hub geometry. It is evident, though, that even now this coupling is significant only among close neighbors, and the scattering matrices are again almost banded. Large off-diagonal elements usually correspond to evanescent modes.

Finally, Fig. 18 and 19 show the effect of the grooves (or, equivalently the blades) in the termination. Three curves are compared to each other for each polarization. The first one corresponds to a simple hub geometry and the two others correspond to the additional presence of blades with varying widths.

6 Appendix I: Closed Form Expressions for the Coefficients of the Mode Matching System of Equations (Cylindrical Hub Termination)

The quantities defined in eq. (59)-(79) can be evaluated in closed form by use of properties of Bessel functions. Particularly useful in the evaluation is eq. (11.3.29), p. 484 of [11]. By defining the following functions:

$$\Omega_n^{(11)}(x;\alpha) \equiv \frac{\alpha x}{2(\alpha^2-1)}\left[\alpha J_n(\alpha x) J_{n-1}(x) - J_{n-1}(\alpha x) J_n(x)\right] + + \frac{\alpha x}{2(\alpha^2-1)}\left[\alpha J_{n+2}(\alpha x) J_{n+1}(x) - J_{n+1}(\alpha x) J_{n+2}(x)\right], \quad \text{if} \quad n \neq 0 \tag{139}$$

$$\Omega_0^{(11)}(x;\alpha) \equiv \frac{2\alpha x}{\alpha^2-1}\left[\alpha J_2(\alpha x) J_1(x) - J_1(\alpha x) J_2(x)\right], \quad \text{if} \quad n = 0 \tag{140}$$

$$\Omega_n^{(12)}(x;\alpha) \equiv \frac{\alpha x}{2(\alpha^2-1)}\left[\alpha J_n(\alpha x) Y_{n-1}(x) - J_{n-1}(\alpha x) Y_n(x)\right] + + \frac{\alpha x}{2(\alpha^2-1)}\left[\alpha J_{n+2}(\alpha x) Y_{n+1}(x) - J_{n+1}(\alpha x) Y_{n+2}(x)\right], \quad \text{if} \quad n \neq 0 \tag{141}$$

$$\Omega_0^{(12)}(x;\alpha) \equiv \frac{2\alpha x}{\alpha^2-1}\left[\alpha J_2(\alpha x) Y_1(x) - J_1(\alpha x) Y_2(x)\right], \quad \text{if} \quad n = 0 \tag{142}$$

the following equalities hold true:

$$
\begin{aligned}
R^{TM}_{mq,np} &= N^{TM}_{1,np} N^{TM}_{2,nq} \pi \delta_{mn} \cdot \\
&\cdot \left\{ Y_n\left(\gamma^{TM}_{2,nq} a\right) \left[\Omega^{(11)}_n \left(\gamma^{TM}_{2,nq} b; \frac{\gamma^{TM}_{1,np}}{\gamma^{TM}_{2,nq}} \right) - \Omega^{(11)}_n \left(\gamma^{TM}_{2,nq} a; \frac{\gamma^{TM}_{1,np}}{\gamma^{TM}_{2,nq}} \right) \right] - \right. \\
&- \left. J_n\left(\gamma^{TM}_{2,nq} a\right) \left[\Omega^{(12)}_n \left(\gamma^{TM}_{2,nq} b; \frac{\gamma^{TM}_{1,np}}{\gamma^{TM}_{2,nq}} \right) - \Omega^{(12)}_n \left(\gamma^{TM}_{2,nq} a; \frac{\gamma^{TM}_{1,np}}{\gamma^{TM}_{2,nq}} \right) \right] \right\} \quad (143) \\
P^{TM}_{mq,np} &= \frac{\beta^{TM}_{1,np}}{\omega\epsilon} \frac{\beta^{TM}_{2,mq}}{\omega\epsilon} R^{TM}_{mq,np} \quad (144) \\
Q^{TM}_{mq,np} &= 0 \quad (145) \\
S^{TM}_{mq,np} &= 0 \quad (146) \\
R^{TE}_{mq,np} &= N^{TM}_{1,np} N^{TE}_{2,nq} \pi \delta_{mn} \frac{\beta^{TE}_{2,nq}}{\omega\mu} n \left\{ \begin{array}{c} -1 \\ 1 \end{array} \right\} J_n\left(\gamma^{TM}_{1,np} a\right) \frac{2}{\pi \gamma^{TE}_{2,nq} a} \quad (147) \\
P^{TE}_{mq,np} &= Z^2 \frac{\beta^{TM}_{1,np}}{\beta^{TE}_{2,nq}} R^{TE}_{mq,np} \quad (148) \\
Q^{TE}_{mq,np} &= N^{TE}_{1,np} N^{TE}_{2,nq} \pi \delta_{mn} \cdot \\
&\cdot \left\{ Y'_n\left(\gamma^{TE}_{2,nq} a\right) \left[\Omega^{(11)}_n \left(\gamma^{TE}_{2,nq} b; \frac{\gamma^{TE}_{1,np}}{\gamma^{TE}_{2,nq}} \right) - \Omega^{(11)}_n \left(\gamma^{TE}_{2,nq} a; \frac{\gamma^{TE}_{1,np}}{\gamma^{TE}_{2,nq}} \right) \right] - \right. \\
&- \left. J'_n\left(\gamma^{TE}_{2,nq} a\right) \left[\Omega^{(12)}_n \left(\gamma^{TE}_{2,nq} b; \frac{\gamma^{TE}_{1,np}}{\gamma^{TE}_{2,nq}} \right) - \Omega^{(12)}_n \left(\gamma^{TE}_{2,nq} a; \frac{\gamma^{TE}_{1,np}}{\gamma^{TE}_{2,nq}} \right) \right] \right\} \quad (149) \\
S^{TE}_{mq,np} &= \frac{\beta^{TE}_{1,np}}{\omega\mu} \frac{\beta^{TE}_{2,mq}}{\omega\mu} Q^{TE}_{mq,np} \quad (150) \\
R^{TEM}_{00,np} &= -N^{TM}_{1,np} N^{TEM}_2 \delta_{n0} \frac{2\pi}{Z} J_0\left(\gamma^{TM}_{1,0p} a\right) \quad (151) \\
P^{TEM}_{00,np} &= Z \frac{\beta^{TM}_{1,0p}}{\omega\epsilon} R^{TEM}_{00,np} \quad (152)
\end{aligned}
$$

$$S_{00,np}^{TEM} = 0 \tag{153}$$

$$Q_{00,np}^{TEM} = 0 \tag{154}$$

where δ_{mn} is the Kronecker delta and Z is the intrinsic impedance of the medium.

7 Appendix II: Modes in a Cylindrical Sector

The geometry of the problem is depicted in Fig. 9. For the TM modes we assume a magnetic vector potential of the form

$$\mathbf{A}^{TM} = \mathbf{u}_z \mu \psi^{TM} \tag{155}$$

Using the method of seperation of variables, and setting

$$\psi(\rho, \phi, z) = R(\rho)\Phi(\phi)Z(z) \tag{156}$$

Helmholtz's equation yields

$$\rho \frac{d}{d\rho}\left(\rho \frac{dR}{d\rho}\right) + \left[(\gamma\rho)^2 - \nu^2\right] R = 0 \tag{157}$$

$$\frac{d^2\Phi}{d\phi^2} + \nu^2 \Phi = 0 \tag{158}$$

$$\frac{d^2Z}{dz^2} + \beta^2 Z = 0 \tag{159}$$

$$\gamma^2 + \beta^2 = k^2 \tag{160}$$

Evidently, from (158)

$$\Phi(\phi) = c_1 \cos \nu\phi + c_2 \sin \nu\phi \tag{161}$$

and since both E_ρ and E_ϕ must vanish at $\phi = 0$ and $\phi = \phi_w$, it follows that

$$c_1 = 0 \tag{162}$$

$$\nu = \frac{m\pi}{\phi_w} \qquad \forall m \in \mathbf{Z} \tag{163}$$

Moreover, (157) implies

$$R(\rho) = b_1 J_\nu(\gamma\rho) + b_2 Y_\nu(\gamma\rho) \tag{164}$$

and we require that E_ϕ and E_z to vanish at $\rho = a$ and $\rho = b$. Hence

$$b_1 J_\nu(\gamma a) + b_2 Y_\nu(\gamma a) = 0 \tag{165}$$

$$b_1 J_\nu(\gamma b) + b_2 Y_\nu(\gamma b) = 0 \tag{166}$$

and since a nontrivial solution is saught for the b's, the determinant of (165), (166) must vanish. Therefore

$$J_\nu(\gamma a)Y_\nu(\gamma b) - J_\nu(\gamma b)Y_\nu(\gamma a) = 0 \tag{167}$$

The latter is the characteristic equation which yields the eigenvalues γ_{mq}, $, q \in \mathbf{N}$ of the problem. Finally, from (159)

$$Z(z) = \kappa_1 e^{j\beta z} + \kappa_2 e^{-j\beta z} \tag{168}$$

In summary, the mq^{th} mode can be expressed as

$$\begin{aligned} \psi_{mq}^{TM} &= \left[Y_\nu(\gamma_{mq}^{TM} a)J_\nu(\gamma_{mq}^{TM}\rho) - J_\nu(\gamma_{mq}^{TM} a)Y_\nu(\gamma_{mq}^{TM}\rho)\right] \cdot \\ &\quad \cdot \; e^{\pm j\beta_{mq}^{TM} z} \sin\nu\phi \qquad (169) \\ \nu &= \frac{m\pi}{\phi_w} \qquad \forall m \in \mathbf{N}_0 \qquad (170) \end{aligned}$$

where γ_{mq}^{TM} is the q^{th} root of the equation

$$J_\nu(\gamma_{mq}^{TM} a)Y_\nu(\gamma_{mq}^{TM} b) - J_\nu(\gamma_{mq}^{TM} b)Y_\nu(\gamma_{mq}^{TM} a) = 0 \tag{171}$$

and

$$(\gamma_{mq}^{TM})^2 + (\beta_{mq}^{TM})^2 = k^2 \tag{172}$$

In a similar way, the TE modes are given by

$$\begin{aligned} \psi_{mq}^{TE} &= \left[Y'_\nu(\gamma_{mq}^{TE}a)J_\nu(\gamma_{mq}^{TE}\rho) - J'_\nu(\gamma_{mq}^{TE}a)Y_\nu(\gamma_{mq}^{TE}\rho)\right] \cdot \\ &\quad \cdot \ \mathrm{e}^{\pm j\beta_{mq}^{TE}z}\cos\nu\phi \end{aligned} \tag{173}$$

$$\nu = \frac{m\pi}{\phi_w} \qquad \forall m \in \mathbf{N}_0 \tag{174}$$

where γ_{mq}^{TE} is the q^{th} root of the equation

$$J'_\nu(\gamma_{mq}^{TE}a)Y'_\nu(\gamma_{mq}^{TE}b) - J'_\nu(\gamma_{mq}^{TE}b)Y'_\nu(\gamma_{mq}^{TE}a) = 0 \tag{175}$$

and

$$(\gamma_{mq}^{TE})^2 + (\beta_{mq}^{TE})^2 = k^2 \tag{176}$$

8 Appendix III: Compact Expressions for the Coefficients of the Mode Matching System of Equations (Groove Array Termination)

As opposed to the cylindrical hub termination, the coefficients of the matrices involved in the mode-matching system of equations cannot be evaluated in closed form. The ϕ integration can be performed analytically, but the ρ integration has to be carried out numerically. To express the coefficients in a compact form, it is convenient to define the following quantities and functions ($\kappa, m, n \in \mathbf{N}_0, \nu = m\pi/\phi_w$):

$$\begin{aligned}
I^{(1)}_{\kappa,nm} &\equiv \int_{\phi_\kappa}^{\phi_\kappa+\phi_w} \cos n\phi \cos\left[\nu\left(\phi-\phi_\kappa\right)\right] d\phi = \\
&= \frac{\phi_w}{2}\mathrm{sinc}\left(\frac{n+\nu}{2}\phi_w\right)\cos\left(\frac{n+\nu}{2}\phi_w + n\phi_\kappa\right) + \\
&+ \frac{\phi_w}{2}\mathrm{sinc}\left(\frac{n-\nu}{2}\phi_w\right)\cos\left(\frac{n-\nu}{2}\phi_w + n\phi_\kappa\right) \qquad (177) \\
I^{(2)}_{\kappa,nm} &\equiv \int_{\phi_\kappa}^{\phi_\kappa+\phi_w} \sin n\phi \cos\left[\nu\left(\phi-\phi_\kappa\right)\right] d\phi = \\
&= \frac{\phi_w}{2}\mathrm{sinc}\left(\frac{n+\nu}{2}\phi_w\right)\sin\left(\frac{n+\nu}{2}\phi_w + n\phi_\kappa\right) + \\
&+ \frac{\phi_w}{2}\mathrm{sinc}\left(\frac{n-\nu}{2}\phi_w\right)\sin\left(\frac{n-\nu}{2}\phi_w + n\phi_\kappa\right) \qquad (178) \\
I^{(3)}_{\kappa,nm} &\equiv \int_{\phi_\kappa}^{\phi_\kappa+\phi_w} \cos n\phi \sin\left[\nu\left(\phi-\phi_\kappa\right)\right] d\phi =
\end{aligned}$$

$$= \frac{\phi_w}{2}\mathrm{sinc}\left(\frac{n+\nu}{2}\phi_w\right)\sin\left(\frac{n+\nu}{2}\phi_w + n\phi_\kappa\right) -$$

$$- \frac{\phi_w}{2}\mathrm{sinc}\left(\frac{n-\nu}{2}\phi_w\right)\sin\left(\frac{n-\nu}{2}\phi_w + n\phi_\kappa\right) \tag{179}$$

$$I^{(4)}_{\kappa,nm} \equiv \int_{\phi_\kappa}^{\phi_\kappa+\phi_w} \sin n\phi \sin\left[\nu\left(\phi-\phi_\kappa\right)\right] d\phi =$$

$$= -\frac{\phi_w}{2}\mathrm{sinc}\left(\frac{n+\nu}{2}\phi_w\right)\cos\left(\frac{n+\nu}{2}\phi_w + n\phi_\kappa\right) +$$

$$+ \frac{\phi_w}{2}\mathrm{sinc}\left(\frac{n-\nu}{2}\phi_w\right)\cos\left(\frac{n-\nu}{2}\phi_w + n\phi_\kappa\right) \tag{180}$$

$$M^{(11)}_{nm}(x_1,x_2;\alpha) \equiv \int_{x_1}^{x_2} J'_n(\alpha\xi)\, J'_\nu(\xi)\, \xi d\xi \tag{181}$$

$$M^{(12)}_{nm}(x_1,x_2;\alpha) \equiv \int_{x_1}^{x_2} J'_n(\alpha\xi)\, Y'_\nu(\xi)\, \xi d\xi \tag{182}$$

$$\Lambda^{(11)}_{nm}(x_1,x_2;\alpha) \equiv \int_{x_1}^{x_2} J_n(\alpha\xi)\, J_\nu(\xi)\, \frac{1}{\xi} d\xi \tag{183}$$

$$\Lambda^{(12)}_{nm}(x_1,x_2;\alpha) \equiv \int_{x_1}^{x_2} J_n(\alpha\xi)\, Y_\nu(\xi)\, \frac{1}{\xi} d\xi \tag{184}$$

$$\Xi^{(11)}_{nm}(x_1,x_2;\alpha) \equiv \int_{x_1}^{x_2} J'_n(\alpha\xi)\, J_\nu(\xi)\, d\xi \tag{185}$$

$$\Xi^{(12)}_{nm}(x_1,x_2;\alpha) \equiv \int_{x_1}^{x_2} J'_n(\alpha\xi)\, Y_\nu(\xi)\, d\xi \tag{186}$$

$$\Psi^{(11)}_{nm}(x_1,x_2;\alpha) \equiv \int_{x_1}^{x_2} J_n(\alpha\xi)\, J'_\nu(\xi)\, d\xi \tag{187}$$

$$\Psi^{(12)}_{nm}(x_1,x_2;\alpha) \equiv \int_{x_1}^{x_2} J_n(\alpha\xi)\, Y'_\nu(\xi)\, d\xi \tag{188}$$

The various coefficients defined in eq. (108)-(119) can be written as

$$
\begin{aligned}
R^{TM}_{\kappa,mq,np} &= N^{TM}_{1,np} N^{TM}_{2,mq} \cdot \\
&\cdot \left\{ Y_\nu\left(\gamma^{TM}_{2,mq} a\right) \left\{ \begin{array}{c} I^{(4)}_{\kappa,nm} \\ I^{(3)}_{\kappa,nm} \end{array} \right\} \frac{\gamma^{TM}_{1,np}}{\gamma^{TM}_{2,mq}} M^{(11)}_{nm}\left(\gamma^{TM}_{2,mq} a, \gamma^{TM}_{2,mq} b; \frac{\gamma^{TM}_{1,np}}{\gamma^{TM}_{2,mq}}\right) + \right. \\
&+ Y_\nu\left(\gamma^{TM}_{2,mq} a\right) \left\{ \begin{array}{c} I^{(1)}_{\kappa,nm} \\ -I^{(2)}_{\kappa,nm} \end{array} \right\} nm \Lambda^{(11)}_{nm}\left(\gamma^{TM}_{2,mq} a, \gamma^{TM}_{2,mq} b; \frac{\gamma^{TM}_{1,np}}{\gamma^{TM}_{2,mq}}\right) - \\
&- J_\nu\left(\gamma^{TM}_{2,mq} a\right) \left\{ \begin{array}{c} I^{(4)}_{\kappa,nm} \\ I^{(3)}_{\kappa,nm} \end{array} \right\} \frac{\gamma^{TM}_{1,np}}{\gamma^{TM}_{2,mq}} M^{(12)}_{nm}\left(\gamma^{TM}_{2,mq} a, \gamma^{TM}_{2,mq} b; \frac{\gamma^{TM}_{1,np}}{\gamma^{TM}_{2,mq}}\right) - \\
&- \left. J_\nu\left(\gamma^{TM}_{2,mq} a\right) \left\{ \begin{array}{c} I^{(1)}_{\kappa,nm} \\ -I^{(2)}_{\kappa,nm} \end{array} \right\} nm \Lambda^{(12)}_{nm}\left(\gamma^{TM}_{2,mq} a, \gamma^{TM}_{2,mq} b; \frac{\gamma^{TM}_{1,np}}{\gamma^{TM}_{2,mq}}\right) \right\} \qquad (189)
\end{aligned}
$$

$$
P^{TM}_{\kappa,mq,np} = \frac{\beta^{TM}_{1,np}}{\omega\epsilon} \frac{\beta^{TM}_{2,mq}}{\omega\epsilon} R^{TM}_{\kappa,mq,np} \qquad (190)
$$

$$
Q^{TM}_{\kappa,mq,np} = 0 \qquad (191)
$$

$$
S^{TM}_{\kappa,mq,np} = 0 \qquad (192)
$$

$$
\begin{aligned}
R^{TE}_{\kappa,mq,np} &= N^{TM}_{1,np} N^{TE}_{2,mq} \frac{\beta^{TE}_{2,mq}}{\omega\mu} \cdot \\
&\cdot \left\{ Y'_\nu\left(\gamma^{TE}_{2,mq} a\right) \left\{ \begin{array}{c} I^{(4)}_{\kappa,nm} \\ I^{(3)}_{\kappa,nm} \end{array} \right\} \nu \frac{\gamma^{TM}_{1,np}}{\gamma^{TE}_{2,mq}} \Xi^{(11)}_{nm}\left(\gamma^{TE}_{2,mq} a, \gamma^{TE}_{2,mq} b; \frac{\gamma^{TM}_{1,np}}{\gamma^{TE}_{2,mq}}\right) + \right. \\
&+ Y'_\nu\left(\gamma^{TE}_{2,mq} a\right) \left\{ \begin{array}{c} I^{(1)}_{\kappa,nm} \\ -I^{(2)}_{\kappa,nm} \end{array} \right\} n \Psi^{(11)}_{nm}\left(\gamma^{TE}_{2,mq} a, \gamma^{TE}_{2,mq} b; \frac{\gamma^{TM}_{1,np}}{\gamma^{TE}_{2,mq}}\right) - \\
&- J'_\nu\left(\gamma^{TE}_{2,mq} a\right) \left\{ \begin{array}{c} I^{(4)}_{\kappa,nm} \\ I^{(3)}_{\kappa,nm} \end{array} \right\} \nu \frac{\gamma^{TM}_{1,np}}{\gamma^{TE}_{2,mq}} \Xi^{(12)}_{nm}\left(\gamma^{TE}_{2,mq} a, \gamma^{TE}_{2,mq} b; \frac{\gamma^{TM}_{1,np}}{\gamma^{TE}_{2,mq}}\right) - \\
&- \left. J'_\nu\left(\gamma^{TE}_{2,mq} a\right) \left\{ \begin{array}{c} I^{(1)}_{\kappa,nm} \\ -I^{(2)}_{\kappa,nm} \end{array} \right\} n \Psi^{(12)}_{nm}\left(\gamma^{TE}_{2,mq} a, \gamma^{TE}_{2,mq} b; \frac{\gamma^{TM}_{1,np}}{\gamma^{TE}_{2,mq}}\right) \right\} \qquad (193)
\end{aligned}
$$

$$
P^{TE}_{\kappa,mq,np} = Z^2 \frac{\beta^{TM}_{1,np}}{\beta^{TE}_{2,mq}} R^{TE}_{\kappa,mq,np} \qquad (194)
$$

$$
Q^{TE}_{\kappa,mq,np} = N^{TE}_{1,np} N^{TE}_{2,mq} \cdot
$$

$$
\begin{aligned}
&\cdot \left\{ Y'_\nu\left(\gamma^{TE}_{2,mq}a\right)\left\{\begin{array}{c} I^{(4)}_{\kappa,nm} \\ I^{(3)}_{\kappa,nm}\end{array}\right\}\frac{\gamma^{TE}_{1,np}}{\gamma^{TE}_{2,mq}}M^{(11)}_{nm}\left(\gamma^{TE}_{2,mq}a,\gamma^{TE}_{2,mq}b;\frac{\gamma^{TE}_{1,np}}{\gamma^{TE}_{2,mq}}\right)+\right. \\
&+ \; Y'_\nu\left(\gamma^{TE}_{2,mq}a\right)\left\{\begin{array}{c} I^{(1)}_{\kappa,nm} \\ -I^{(2)}_{\kappa,nm}\end{array}\right\}nm\Lambda^{(11)}_{nm}\left(\gamma^{TE}_{2,mq}a,\gamma^{TE}_{2,mq}b;\frac{\gamma^{TE}_{1,np}}{\gamma^{TE}_{2,mq}}\right)- \\
&- \; J'_\nu\left(\gamma^{TE}_{2,mq}a\right)\left\{\begin{array}{c} I^{(4)}_{\kappa,nm} \\ I^{(3)}_{\kappa,nm}\end{array}\right\}\frac{\gamma^{TE}_{1,np}}{\gamma^{TE}_{2,mq}}M^{(12)}_{nm}\left(\gamma^{TE}_{2,mq}a,\gamma^{TE}_{2,mq}b;\frac{\gamma^{TE}_{1,np}}{\gamma^{TE}_{2,mq}}\right)- \\
&\left.- \; J'_\nu\left(\gamma^{TE}_{2,mq}a\right)\left\{\begin{array}{c} I^{(1)}_{\kappa,nm} \\ -I^{(2)}_{\kappa,nm}\end{array}\right\}nm\Lambda^{(12)}_{nm}\left(\gamma^{TE}_{2,mq}a,\gamma^{TE}_{2,mq}b;\frac{\gamma^{TE}_{1,np}}{\gamma^{TE}_{2,mq}}\right)\right\} \qquad (195)
\end{aligned}
$$

$$
S^{TE}_{\kappa,mq,np} = \frac{\beta^{TE}_{1,np}}{\omega\mu}\frac{\beta^{TE}_{2,mq}}{\omega\mu}Q^{TE}_{\kappa,mq,np} \qquad (196)
$$

$$
(197)
$$

9 Appendix IV: Explicit Radiation Coefficients for Circular Inlets

In the near zone, there is no simple closed form expression for the radiated field due to an outgoing waveguide mode. However, it is possible to derive closed form expressions for far zone observations. From [5], the far zone field due to each mode is given by

$$
\mathbf{E}_{rad} = \left[E_\theta\left\{\begin{array}{c}\cos n\phi \\ -\sin n\phi\end{array}\right\}\mathbf{u}_\theta + E_\phi\left\{\begin{array}{c}\sin n\phi \\ \cos n\phi\end{array}\right\}\mathbf{u}_\phi\right]\frac{\mathrm{e}^{-jkr}}{r} \qquad (198)
$$

$$
E_\theta = E_{\theta k} + E_{\theta u} \qquad (199)
$$

$$
E_\phi = E_{\phi k} + E_{\phi u} \qquad (200)
$$

where $E_{\theta k}, E_{\phi k}$ are associated with the contribution from the Kirchhoff integral and $E_{\theta u}, E_{\phi u}$ correspond to the contribution from the equivalent fringe rim current (Ufimtsef type). Explicit expressions of $E_{\theta k}, E_{\phi k}, E_{\theta u}, E_{\phi u}$ are given below:

TM_{np} modes:

$$
\begin{aligned}
E_{\theta k} &= j^n k N_{1,np}^{TM} \gamma_{1,np}^{TM} b \cdot \\
&\cdot \frac{\sin\theta}{2\left(\cos\psi_{1,np}^{TM} - \cos\theta\right)} J_n'\left(\gamma_{1,np}^{TM} b\right) J_n\left(kb\sin\theta\right) \qquad (201) \\
E_{\phi k} &= 0 \qquad (202) \\
E_{\theta u} &= j^n N_{1,np}^{TM} J_n'\left(\gamma_{1,np}^{TM} b\right) \frac{\cos\left(\theta/2\right) - \cos\left(\psi_{1,np}^{TM}/2\right)}{\cos\psi_{1,np}^{TM} - \cos\theta} \cdot \\
&\cdot \left[n^2 \beta_{1,np}^{TM} \sin\frac{\psi_{1,np}^{TM}}{2} \frac{\cot\theta}{kb} J_n\left(kb\sin\theta\right) + \right. \\
&+ \left. k\gamma_{1,np}^{TM} b \sin\frac{\theta}{2} J_n''\left(kb\sin\theta\right)\right] \qquad (203) \\
E_{\phi u} &= -j^n N_{1,np}^{TM} n J_n'\left(\gamma_{1,np}^{TM} b\right) \frac{\cos\left(\theta/2\right) - \cos\left(\psi_{1,np}^{TM}/2\right)}{\cos\psi_{1,np}^{TM} - \cos\theta} \cdot \\
&\cdot \left\{\beta_{1,np}^{TM} \sin\frac{\psi_{1,np}^{TM}}{2} J_n'\left(kb\sin\theta\right) + \right.
\end{aligned}
$$

$$+ \quad k\gamma_{1,np}^{TM} b \sin\frac{\theta}{2}\frac{\cot\theta}{kb}\left[J_n'\left(kb\sin\theta\right) - \frac{J_n\left(kb\sin\theta\right)}{kb\sin\theta}\right]\Bigg\} \qquad (204)$$

TE_{np} modes:

$$E_{\theta k} = j^n kZN_{1,np}^{TE} n \cdot$$
$$\cdot \quad \frac{1+\cos\theta\cos\psi_{1,np}^{TE}}{2\sin\theta} J_n\left(\gamma_{1,np}^{TE} b\right) J_n\left(kb\sin\theta\right) \qquad (205)$$

$$E_{\phi k} = j^n kZN_{1,np}^{TE}\gamma_{1,np}^{TE} b \cdot$$
$$\cdot \quad \frac{\sin\psi_{1,np}^{TE}}{2\left(\cos\psi_{1,np}^{TE} - \cos\theta\right)} J_n\left(\gamma_{1,np}^{TE} b\right) J_n'\left(kb\sin\theta\right) \qquad (206)$$

$$E_{\theta u} = j^n ZN_{1,np}^{TE} n J_n\left(\gamma_{1,np}^{TE} b\right) \frac{\cos\left(\theta/2\right) - \cos\left(\psi_{1,np}^{TE}/2\right)}{\cos\psi_{1,np}^{TE} - \cos\theta} \cdot$$
$$\cdot \quad \Bigg\{\beta_{1,np}^{TE}\sin\frac{\theta}{2} J_n''\left(kb\sin\theta\right) -$$
$$- \quad k\gamma_{1,np}^{TE} b\sin\frac{\psi_{1,np}^{TE}}{2}\frac{\cot\theta}{kb} J_n\left(kb\sin\theta\right)\Bigg\} \qquad (207)$$

$$E_{\phi u} = j^n ZN_{1,np}^{TE} J_n\left(\gamma_{1,np}^{TE} b\right) \frac{\cos\left(\theta/2\right) - \cos\left(\psi_{1,np}^{TE}/2\right)}{\cos\psi_{1,np}^{TE} - \cos\theta} \cdot$$
$$\cdot \quad \Bigg\{k\gamma_{1,np}^{TE} b\sin\frac{\psi_{1,np}^{TE}}{2} J_n'\left(kb\sin\theta\right) -$$
$$- \quad n^2\beta_{1,np}^{TE}\sin\frac{\theta}{2}\frac{\cot\theta}{kb}\left[J_n'\left(kb\sin\theta\right) - \frac{J_n\left(kb\sin\theta\right)}{kb\sin\theta}\right]\Bigg\} \qquad (208)$$

where, by definition

$$\cos \psi_{1,np}^{TM,TE} \equiv \frac{\beta_{1,np}^{TM,TE}}{k} \tag{209}$$

10 Acknowledgement

The authors are indebted to Dr. R. J. Burkholder of the Ohio State University for the supply of several numerical results based on the Hybrid Moment-Method Modal Technique.

References

[1] T.W Johnson and D. L. Moffat, "Electromagnetic Scattering by open Circular Waveguides", Technical Report 710816-9, The Ohio State University, ElectroScience Laboratory, Columbus OH, December 1980.

[2] R. Mittra and S.W. Lee, *Analytical Techniques in the Theory of Guided Waves*, Mac Millan, 1971.

[3] Ching-Chao Huang, "Ray Analysis of EM Backscatter from a Cavity Configuration", Ph.D. Dissertation, The Ohio State University, ElectroScience Laboratory, Columbus OH, 1982.

[4] Ayhan Altintas, "Electromagnetic Scattering from a Class of Open-Ended Waveguide Discontinuities", Ph.D. Dissertation, The Ohio State University, ElectroScience Laboratory, Columbus OH, 1986.

[5] P. H. Pathak, C. W. Chuang, M. C. Liang, "Inlet Modeling Studies", Technical Report 717674-1, The Ohio State University, ElectroScience Laboratory, Columbus OH, October 1980.

[6] R. J. Burkholder and P. H. Pathak, "High Frequency Asymptotic Methods for Analyzing the EM Scattering by Open-Ended Waveguide Cavities", Technical Report 719630-3, The Ohio State University, ElectroScience Laboratory, Columbus OH, September 1989.

[7] P. P. Silvester and R. L. Ferrari, *Finite Elements for Electrical Engineers*, Cambridge, 1986.

[8] R. F. Harrington, *Time-Harmonic Electromagnetic Fields*, Mc Graw-Hill, 1961.

[9] N. Marcuvitz, *Waveguide Handbook*, Krieger, IEE Press, P. Peregrinus Ltd., 1986, pp. 72-77.

[10] R. J. Burkholder, The Ohio State University, ElectroScience Laboratory (personal communication).

[11] M. Abramowitz and I. E. Stegun, *Handbook of Mathematical Functions*, Dover, 1970, p. 484.

99

LIST OF FIGURES:

Polarization).

Figure 8: Amplitudes of the elements of the generalized scattering matrix calculated by Mode Matching for a hub termination with $a = 1.5\lambda, b = 3\lambda, l_1 = 16.595\lambda, l_2 = 1\lambda$.

Modes 1-10: $TM_{0,1}$ to $TM_{0,10}$ ($\propto \cos n\phi$)

Modes 11-20: $TM_{1,1}$ to $TM_{1,10}$ ($\propto \cos n\phi$)

Modes 21-30: $TM_{2,1}$ to $TM_{2,10}$ ($\propto \cos n\phi$)

Modes 31-40: $TE_{0,1}$ to $TE_{0,10}$ ($\propto \sin n\phi$)

Modes 41-50: $TE_{1,1}$ to $TE_{1,10}$ ($\propto \sin n\phi$)

Modes 51-60: $TE_{2,1}$ to $TE_{2,10}$ ($\propto \sin n\phi$)

Figure 9: Amplitudes of the elements of the generalized scattering matrix calculated by Mode Matching for a hub termination with $a = 0.503\lambda, b = 1.66\lambda, l_1 = 16.595\lambda, l_2 = 0.335\lambda$. The mode numbering is identical to Figure 8.

Figure 10: Geometry of the problem (groove array termination). Cross-hatching denotes perfectly conducting surfaces.

Figure 11: Cylindrical sector.

Figure 12: RCS (dB/λ^2) calculated by the Mode Matching Technique for a groove array termination with $a = 1.5\lambda, b = 3\lambda, l_1 = 5\lambda, l_2 = 0.5\lambda, 8$ fins, $\phi_w =$

$40°, \phi_1 = 10°$. (Vertical Polarization).

Figure 13: RCS (dB/λ^2) calculated by the Mode Matching Technique for a groove array termination with $a = 1.5\lambda, b = 3\lambda, l_1 = 5\lambda, l_2 = 0.5\lambda, 8$ fins, $\phi_w = 40°, \phi_1 = 10°$. (Horizontal Polarization).

Figure 14: RCS (dB/λ^2) calculated by the Mode Matching Technique for a groove array termination with $a = 0.5\lambda, b = 1.5\lambda, l_1 = 5\lambda, l_2 = 0.2\lambda, 4$ fins, $\phi_w = 45°, \phi_1 = 0°$. (Vertical Polarization).

Figure 15: RCS (dB/λ^2) calculated by the Mode Matching Technique for a groove array termination with $a = 0.5\lambda, b = 1.5\lambda, l_1 = 5\lambda, l_2 = 0.2\lambda, 4$ fins, $\phi_w = 45°, \phi_1 = 0°$. (Horizontal Polarization).

Figure 16: Amplitudes of the elements of the generalized scattering matrix calculated by Mode Matching for a groove array termination with $a = 1.5\lambda, b = 3\lambda, l_1 = 5\lambda, l_2 = 0.5\lambda, 8$ fins, $\phi_w = 40°, \phi_1 = 10°$.

Modes 1-10: $TM_{0,1}$ to $TM_{0,10}$ ($\propto \cos n\phi$)

Modes 11-20: $TM_{1,1}$ to $TM_{1,10}$ ($\propto \cos n\phi$)

Modes 21-30: $TE_{0,1}$ to $TE_{0,10}$ ($\propto \sin n\phi$)

Modes 31-40: $TE_{1,1}$ to $TE_{1,10}$ ($\propto \sin n\phi$)

Modes 41-50: $TM_{0,1}$ to $TM_{0,10}$ ($\propto \sin n\phi$)

Modes 51-60: $TM_{1,1}$ to $TM_{1,10}$ ($\propto \sin n\phi$)

Modes 61-70: $TE_{0,1}$ to $TE_{0,10}$ ($\propto \cos n\phi$)

Modes 71-80: $TE_{1,1}$ to $TE_{1,10}$ ($\propto \cos n\phi$)

Figure 17: Amplitudes of the elements of the generalized scattering matrix calculated by Mode Matching for a groove array termination with $a = 0.5\lambda, b = 1.5\lambda, l_1 = 5\lambda, l_2 = 0.2\lambda, 4$ fins, $\phi_w = 45^o, \phi_1 = 0^o$.

Modes 1-7: $TM_{0,1}$ to $TM_{0,7}$ ($\propto \cos n\phi$)

Modes 8-14: $TM_{1,1}$ to $TM_{1,7}$ ($\propto \cos n\phi$)

Modes 15-21: $TM_{2,1}$ to $TM_{2,7}$ ($\propto \cos n\phi$)

Modes 22-28: $TE_{0,1}$ to $TE_{0,7}$ ($\propto \sin n\phi$)

Modes 29-35: $TE_{1,1}$ to $TE_{1,7}$ ($\propto \sin n\phi$)

Modes 36-42: $TE_{2,1}$ to $TE_{2,7}$ ($\propto \sin n\phi$)

Modes 43-49: $TM_{0,1}$ to $TM_{0,7}$ ($\propto \sin n\phi$)

Modes 50-56: $TM_{1,1}$ to $TM_{1,7}$ ($\propto \sin n\phi$)

Modes 57-63: $TM_{2,1}$ to $TM_{2,7}$ ($\propto \sin n\phi$)

Modes 64-70: $TE_{0,1}$ to $TE_{0,7}$ ($\propto \cos n\phi$)

Modes 71-77: $TE_{1,1}$ to $TE_{1,7}$ ($\propto \cos n\phi$)

Modes 78-84: $TE_{2,1}$ to $TE_{2,7}$ ($\propto \cos n\phi$)

Figure 18: Effect of the presence of the termination blades on the RCS (measured in dB/λ^2). Dimensions: $a = 1.5\lambda, b = 3\lambda, l_1 = 5\lambda, l_2 = 0.5\lambda, 8$ blades, $\phi_1 =$

0° (Vertical Polarization).

Figure 19: Effect of the presence of the termination blades on the RCS (measured in dB/λ^2). Dimensions: $a = 1.5\lambda, b = 3\lambda, l_1 = 5\lambda, l_2 = 0.5\lambda, 8$ blades, $\phi_1 = 0^{\circ}$ (Horizontal Polarization).

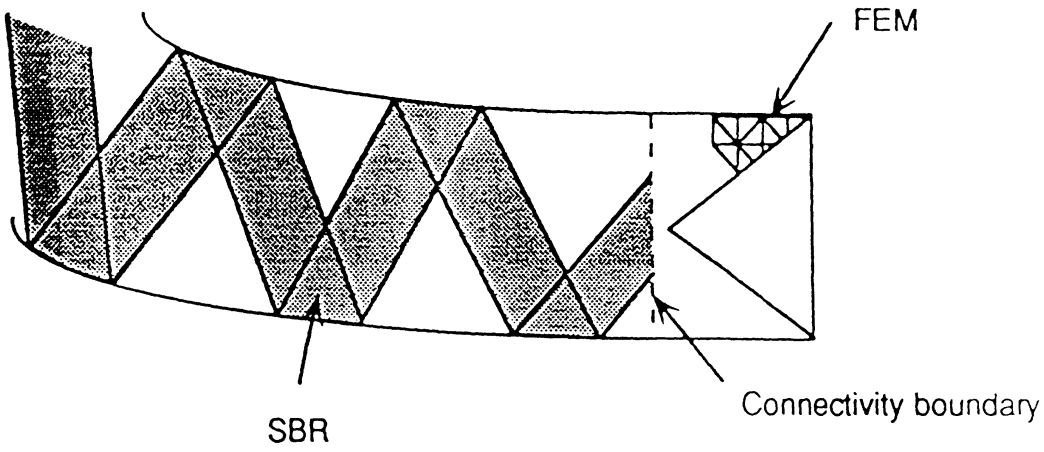

Figure 1: The Finite Element Method combined with the Shooting and Bouncing Ray (SBR) Method.

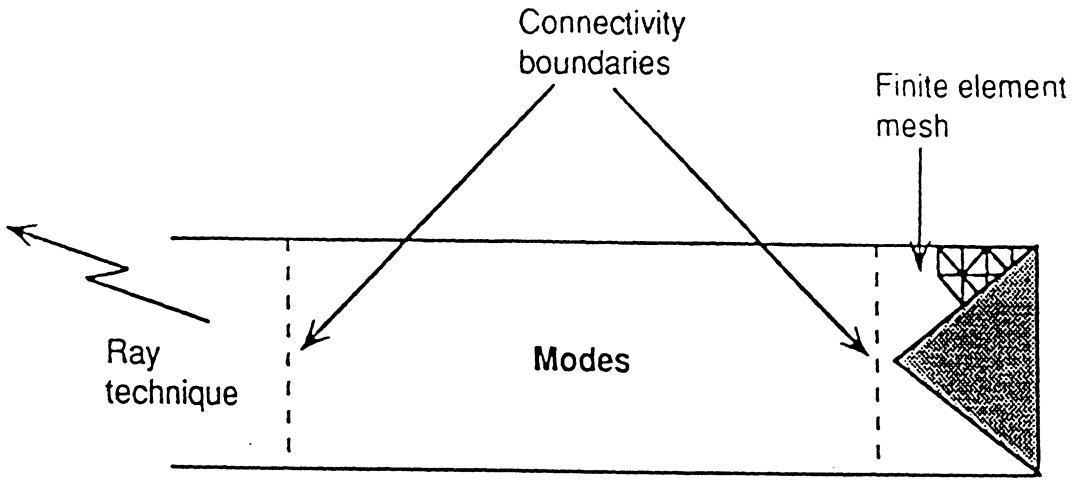

Figure 2: The Finite Element Method combined with Modal and Ray Tracing Methods.

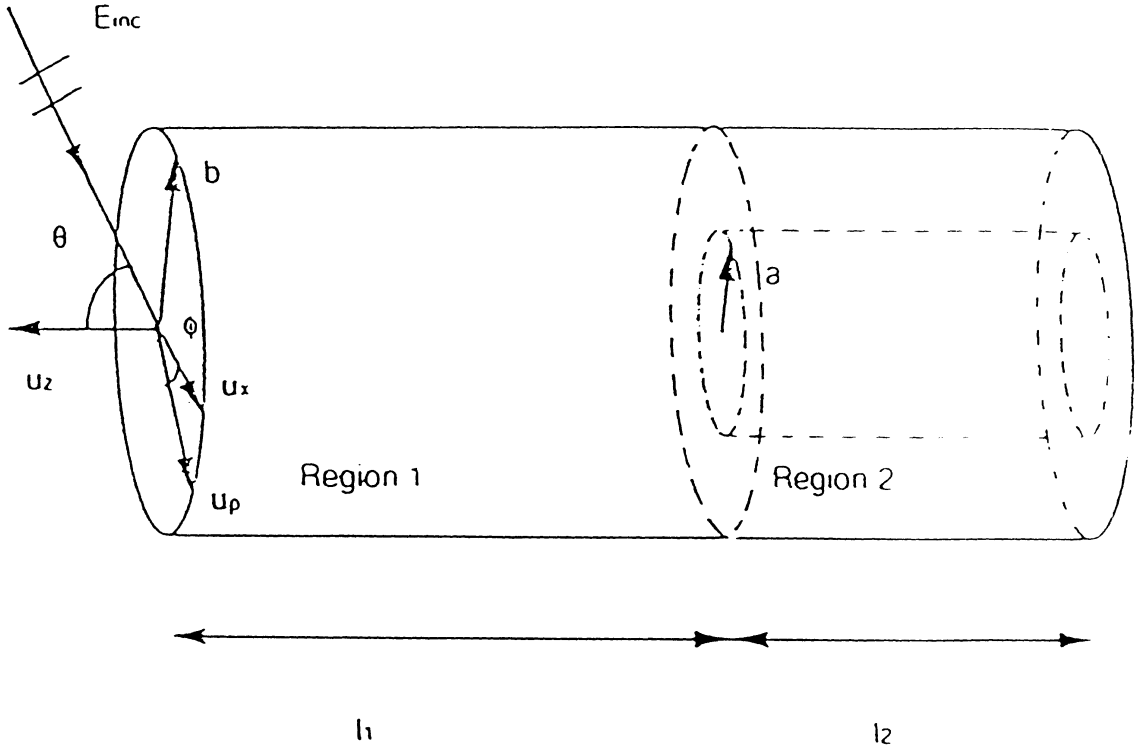

Figure 3: Geometry of the problem (cylindrical hub termination).

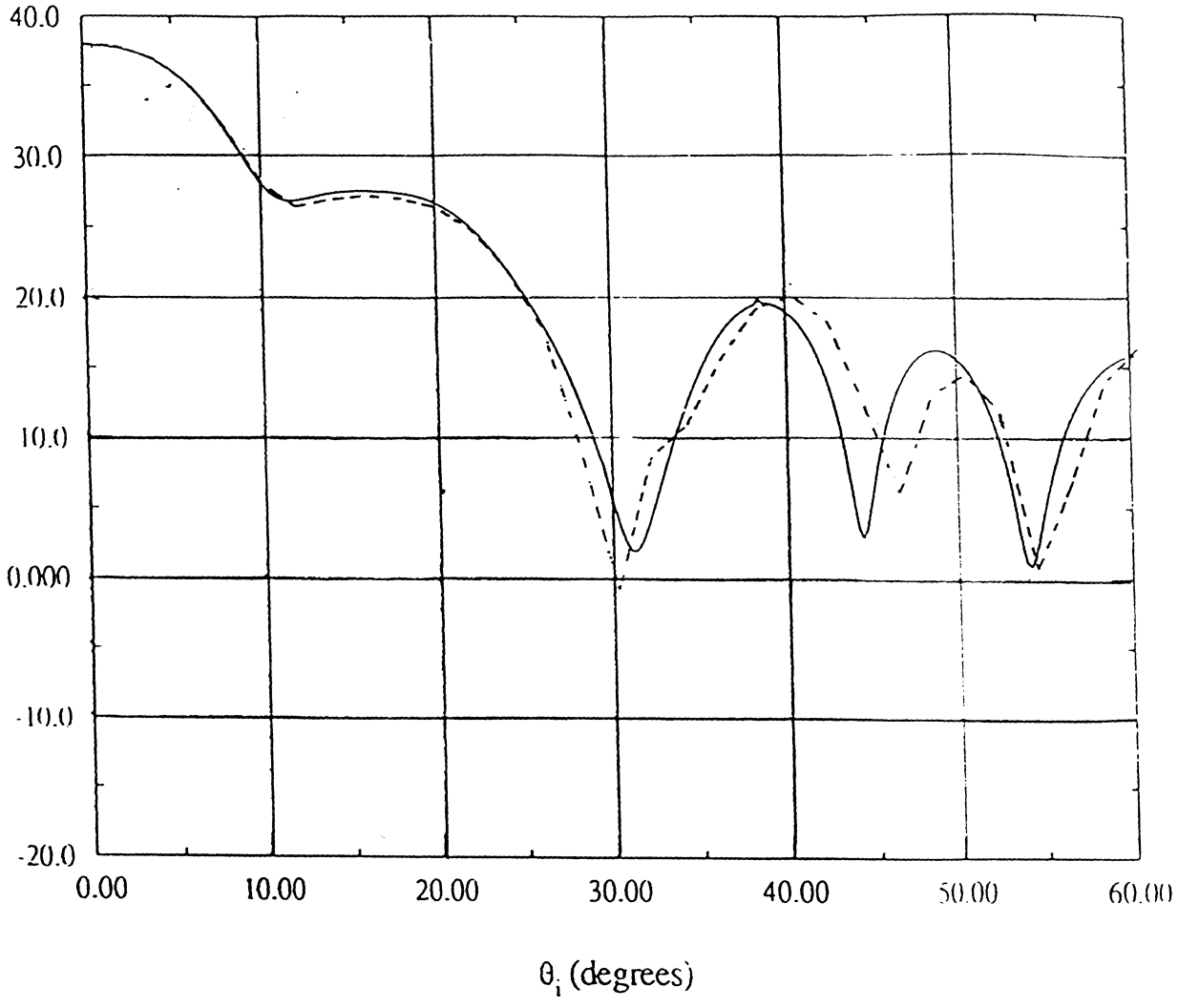

Figure 4: RCS (dB/λ^2) calculated by the Mode Matching Technique (solid line) and the Hybrid Modal Technique (dashed line) for $a = 1.5\lambda, b = 3\lambda, l_1 = 16.595\lambda, l_2 = 1\lambda$ (Vertical Polarization).

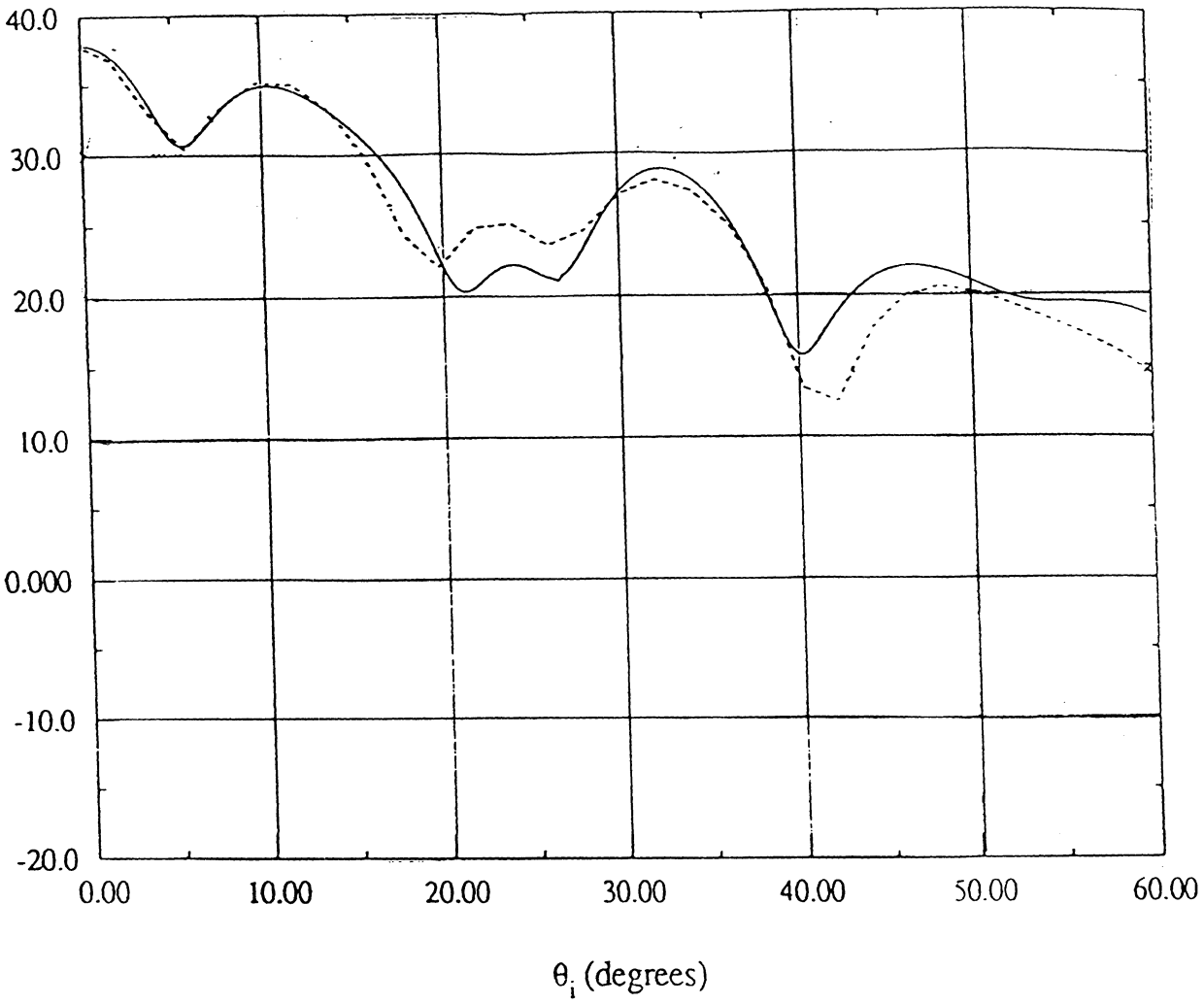

Figure 5: RCS (dB/λ^2) calculated by the Mode Matching Technique (solid line) and the Hybrid Modal Technique (dashed line) for $a = 1.5\lambda, b = 3\lambda, l_1 = 16.595\lambda, l_2 = 1\lambda$ (Horizontal Polarization).

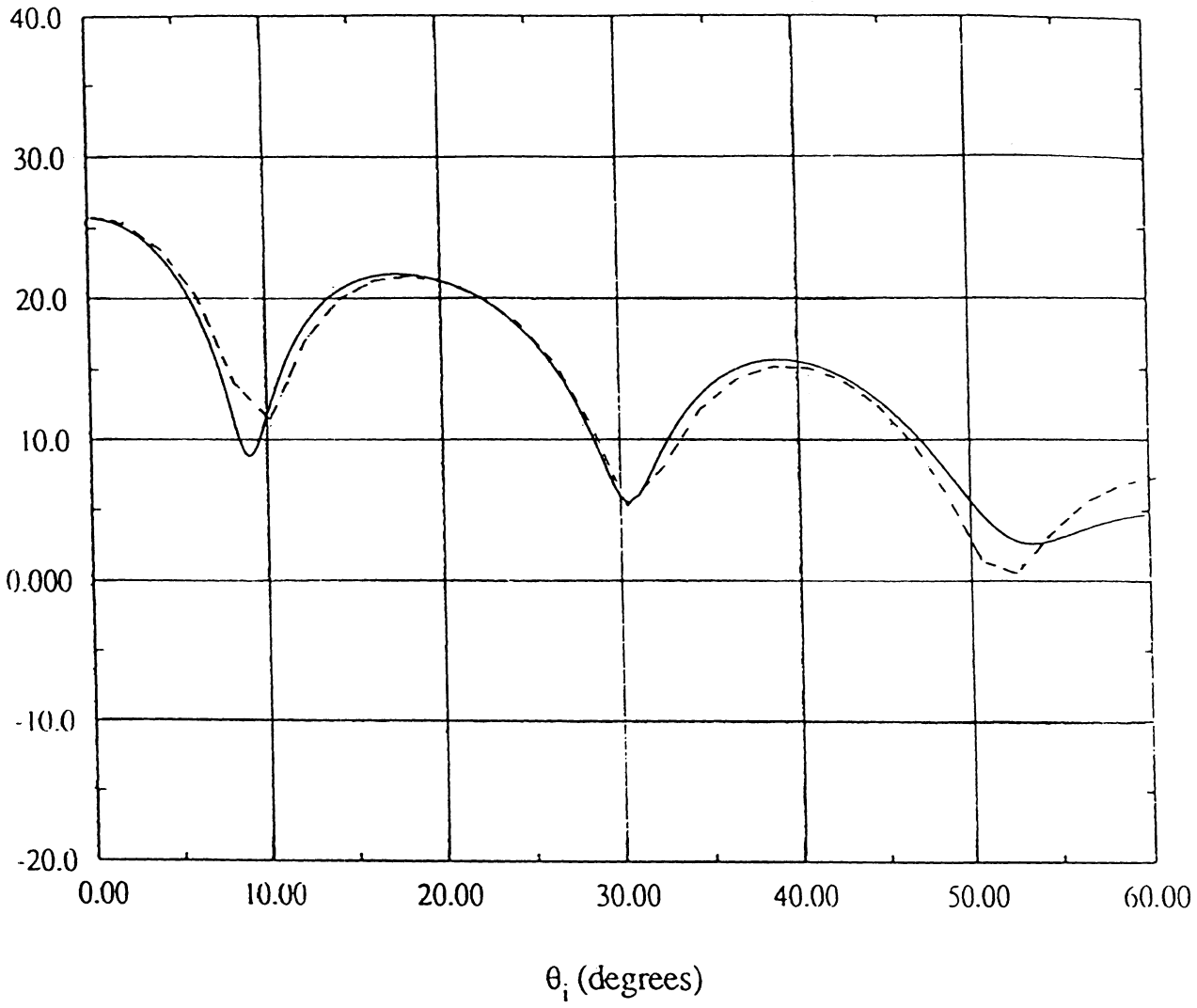

Figure 6: RCS (dB/λ^2) calculated by the Mode Matching Technique (solid line) and the Hybrid Modal Technique (dashed line) for $a = 0.503\lambda, b = 1.66\lambda, l_1 = 16.595\lambda, l_2 = 0.335\lambda$. (Vertical Polarization).

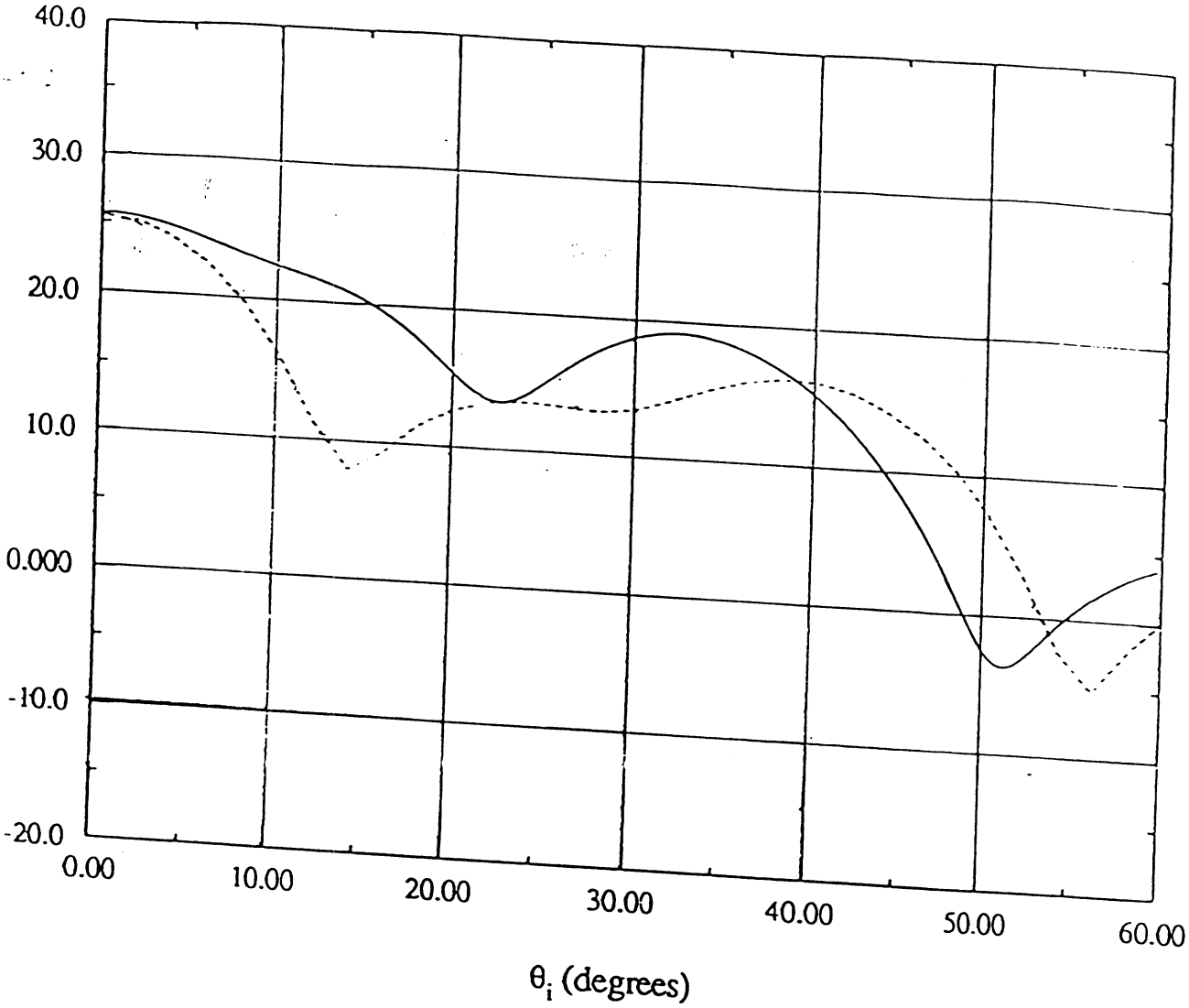

Figure 7: RCS (dB/λ^2) calculated by the Mode Matching Technique (solid line) and the Hybrid Modal Technique (dashed line) for $a = 0.503\lambda, b = 1.66\lambda, l_1 = 16.595\lambda, l_2 = 0.335\lambda$. (Horizontal Polarization).

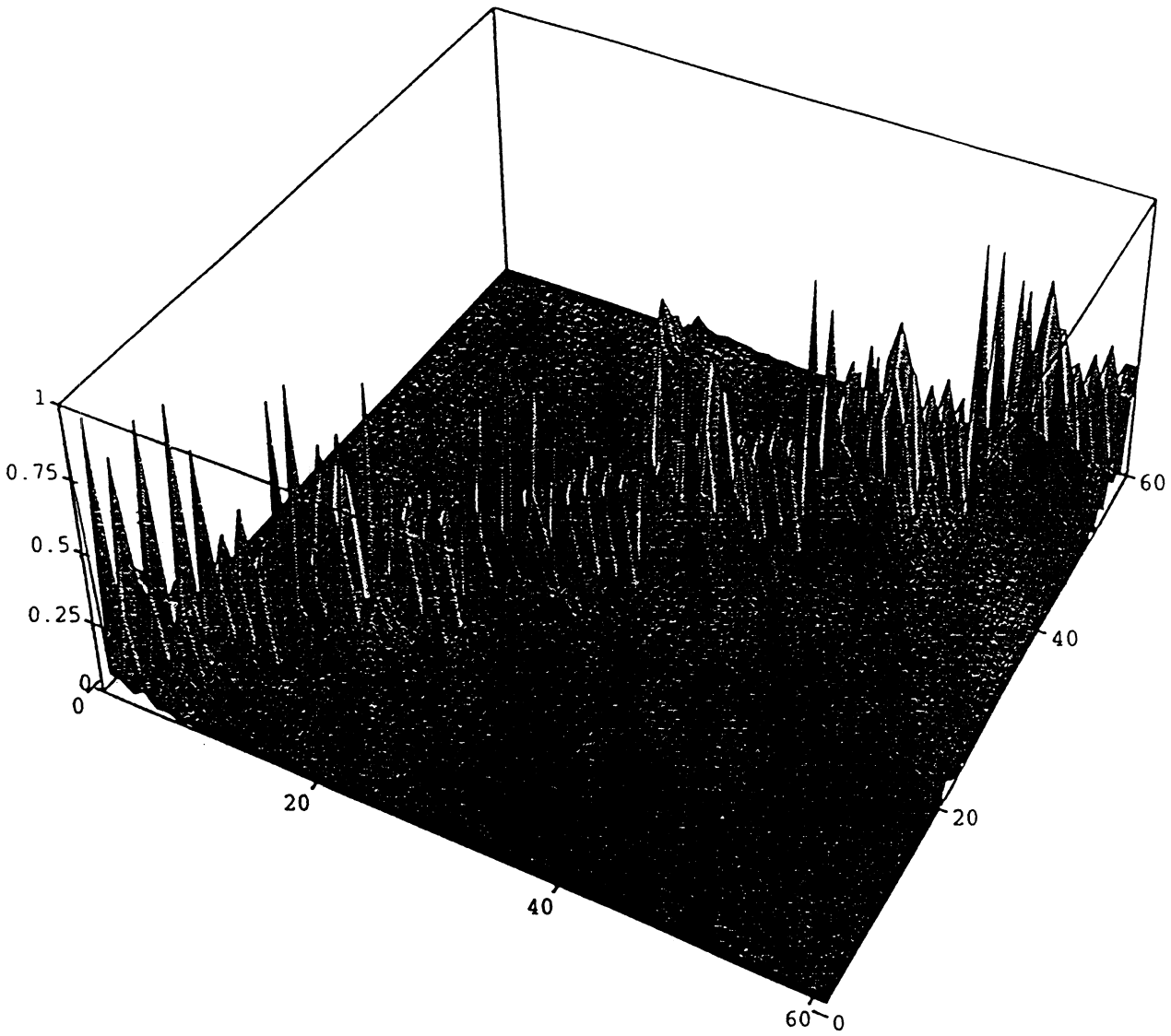

Figure 8: Amplitudes of the elements of the generalized scattering matrix calculated by Mode Matching for a hub termination with $a = 1.5\lambda, b = 3\lambda, l_1 = 16.595\lambda, l_2 = 1\lambda$. (See List of Figures for more details).

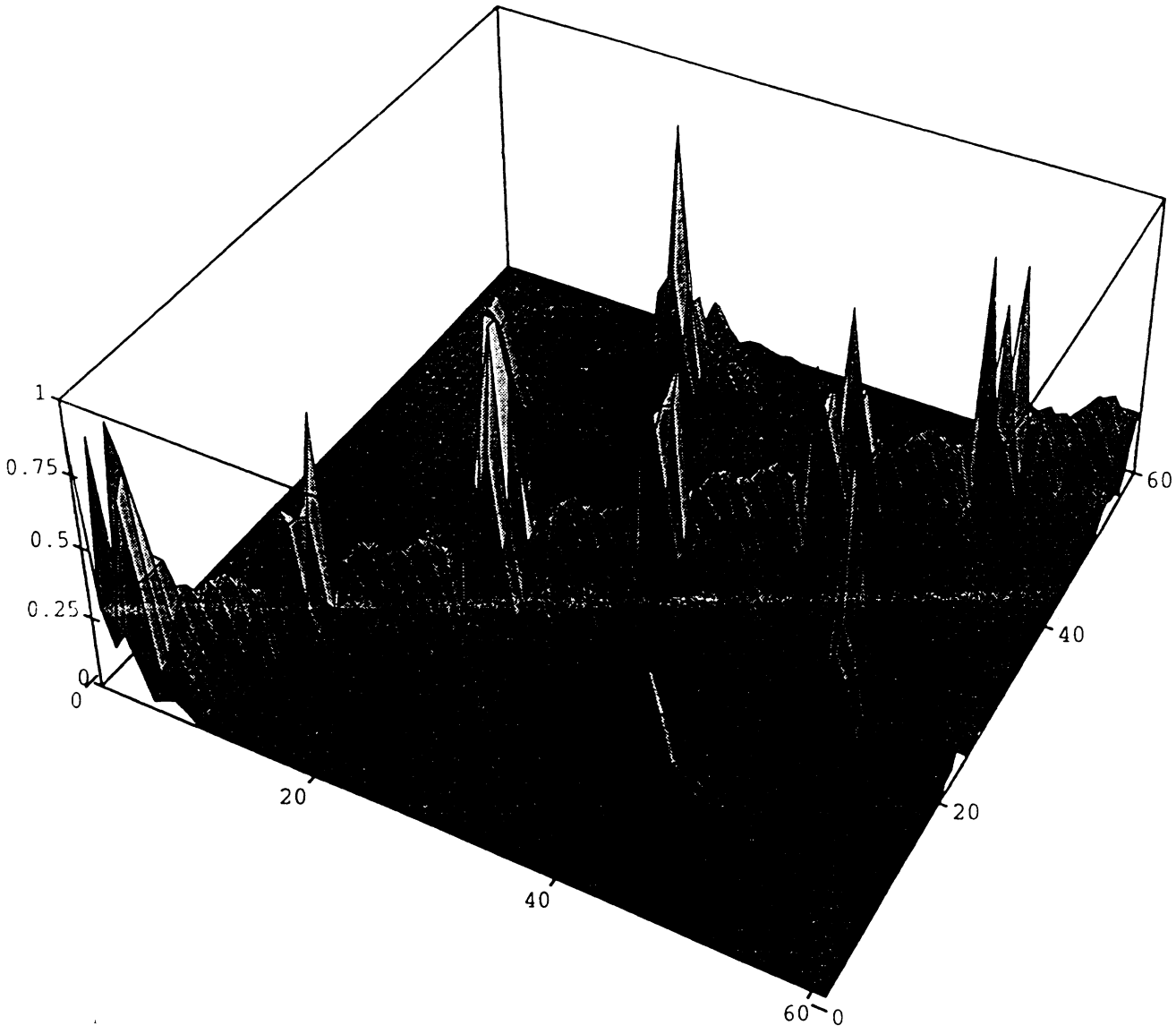

Figure 9: Amplitudes of the elements of the generalized scattering matrix calculated by Mode Matching for a hub termination with $a = 0.503\lambda, b = 1.66\lambda, l_1 = 16.595\lambda, l_2 = 0.335\lambda$. The mode numbering is identical to Figure 8.

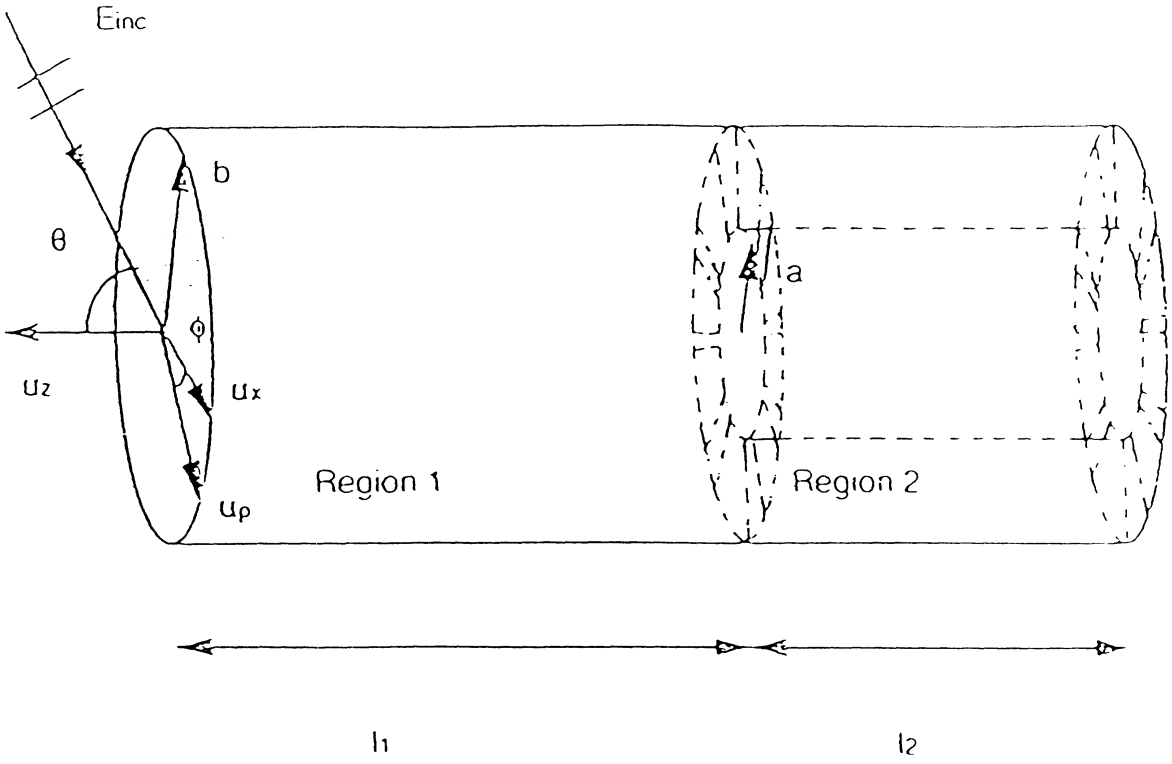

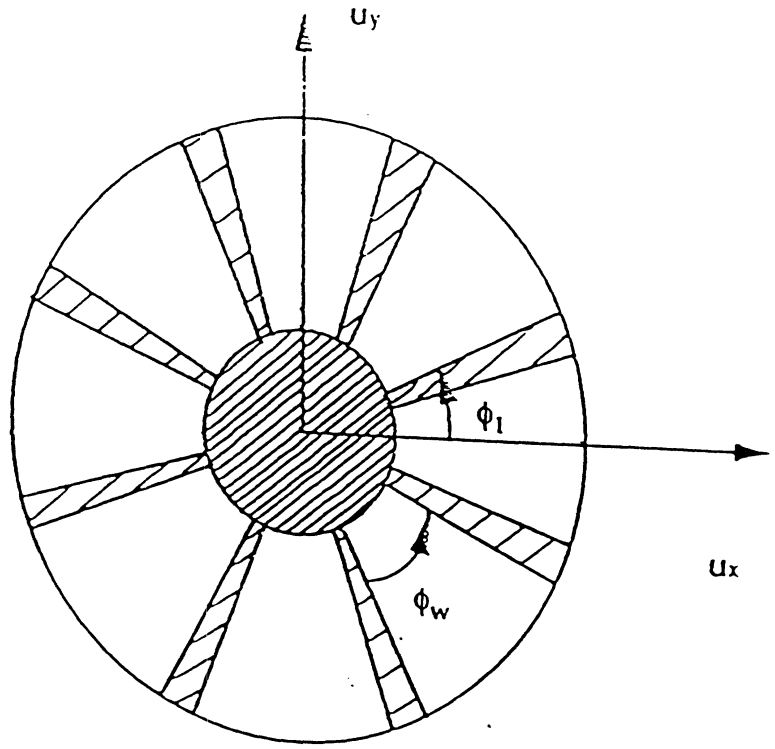

Figure 10: Geometry of the problem (groove array termination). Cross-hatching denotes perfectly conducting surfaces.

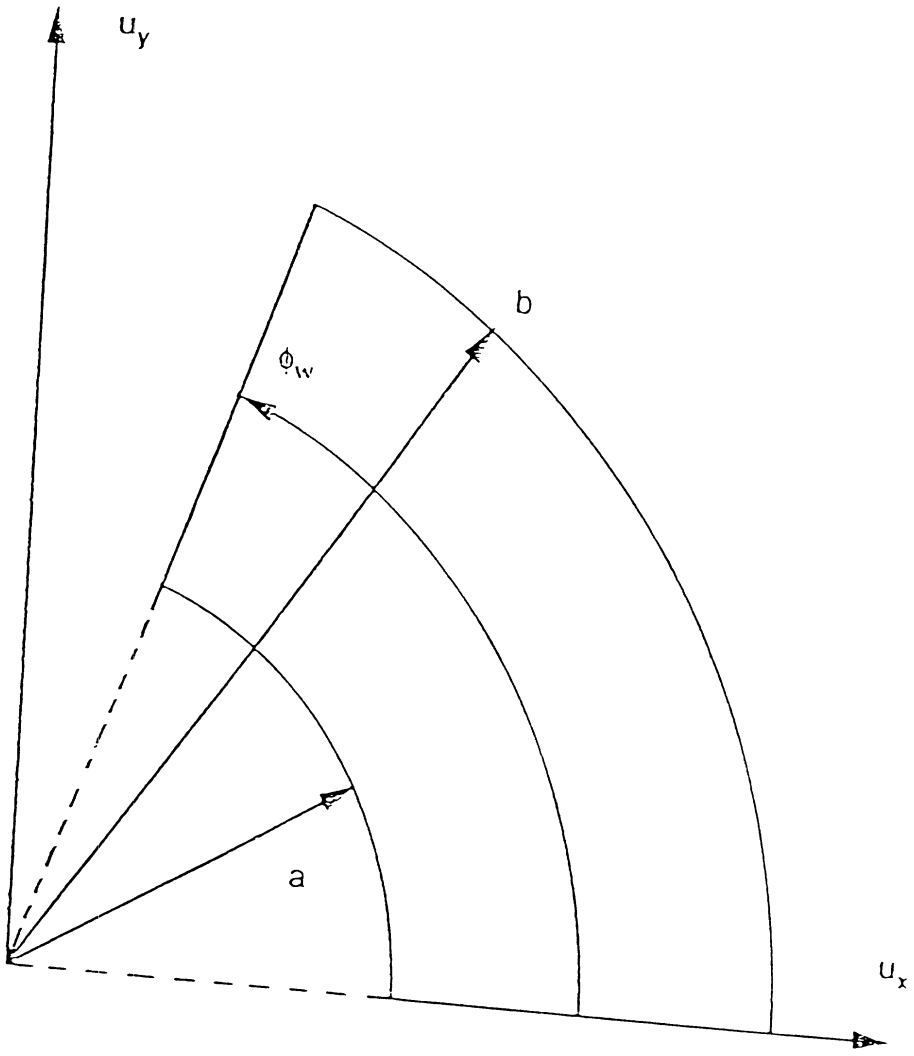

Figure 11: Cylindrical sector.

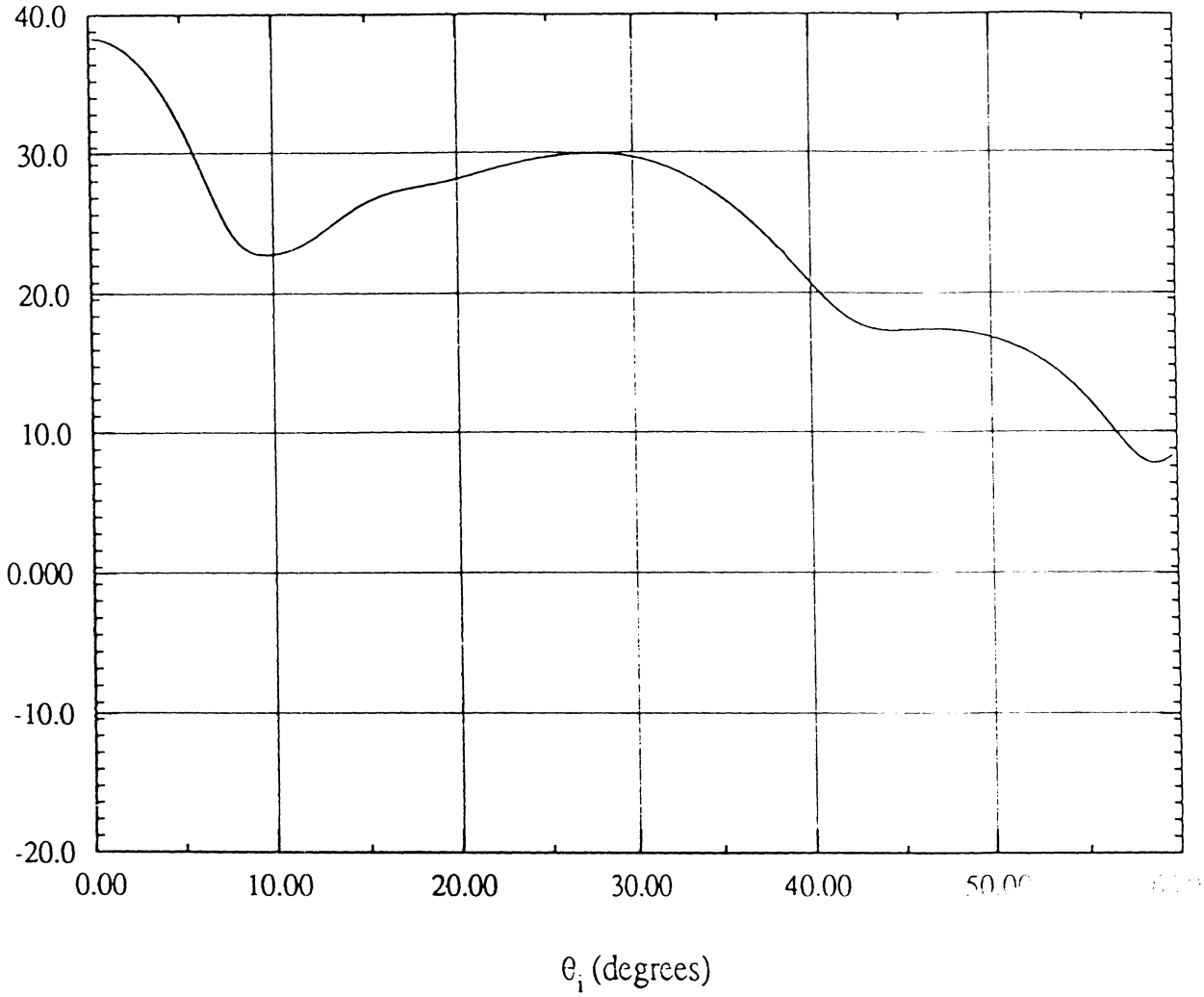

Figure 12: RCS (dB/λ^2) calculated by the Mode Matching Technique for a groove array termination with $a = 1.5\lambda, b = 3\lambda, l_1 = 5\lambda, l_2 = 0.5\lambda, 8$ fins, $\phi_w = 40^o, \phi_1 = 10^o$. (Vertical Polarization).

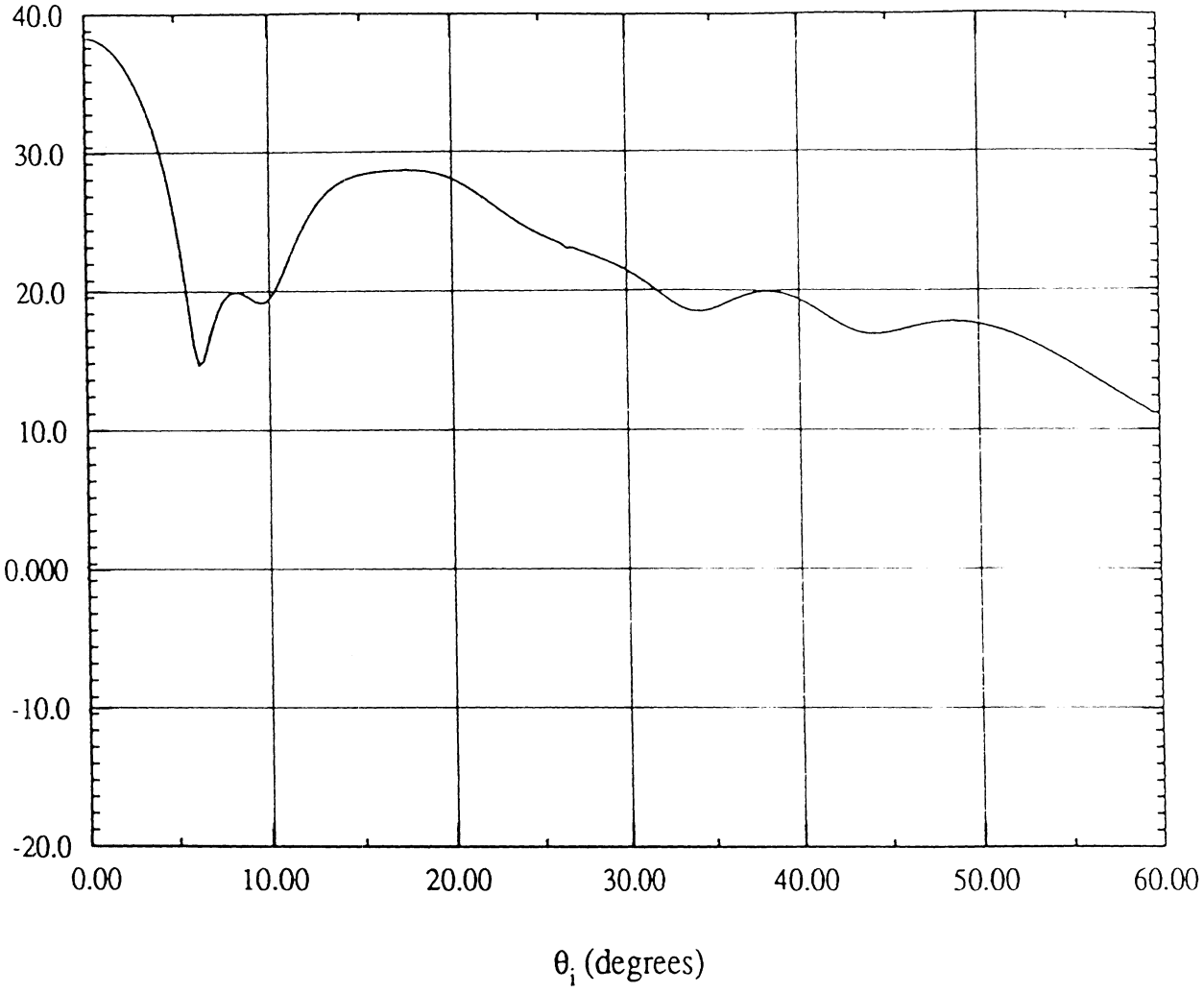

Figure 13: RCS (dB/λ^2) calculated by the Mode Matching Technique for a groove array termination with $a = 1.5\lambda, b = 3\lambda, l_1 = 5\lambda, l_2 = 0.5\lambda, 8$ fins, $\phi_w = 40^o, \phi_1 = 10^o$. (Horizontal Polarization).

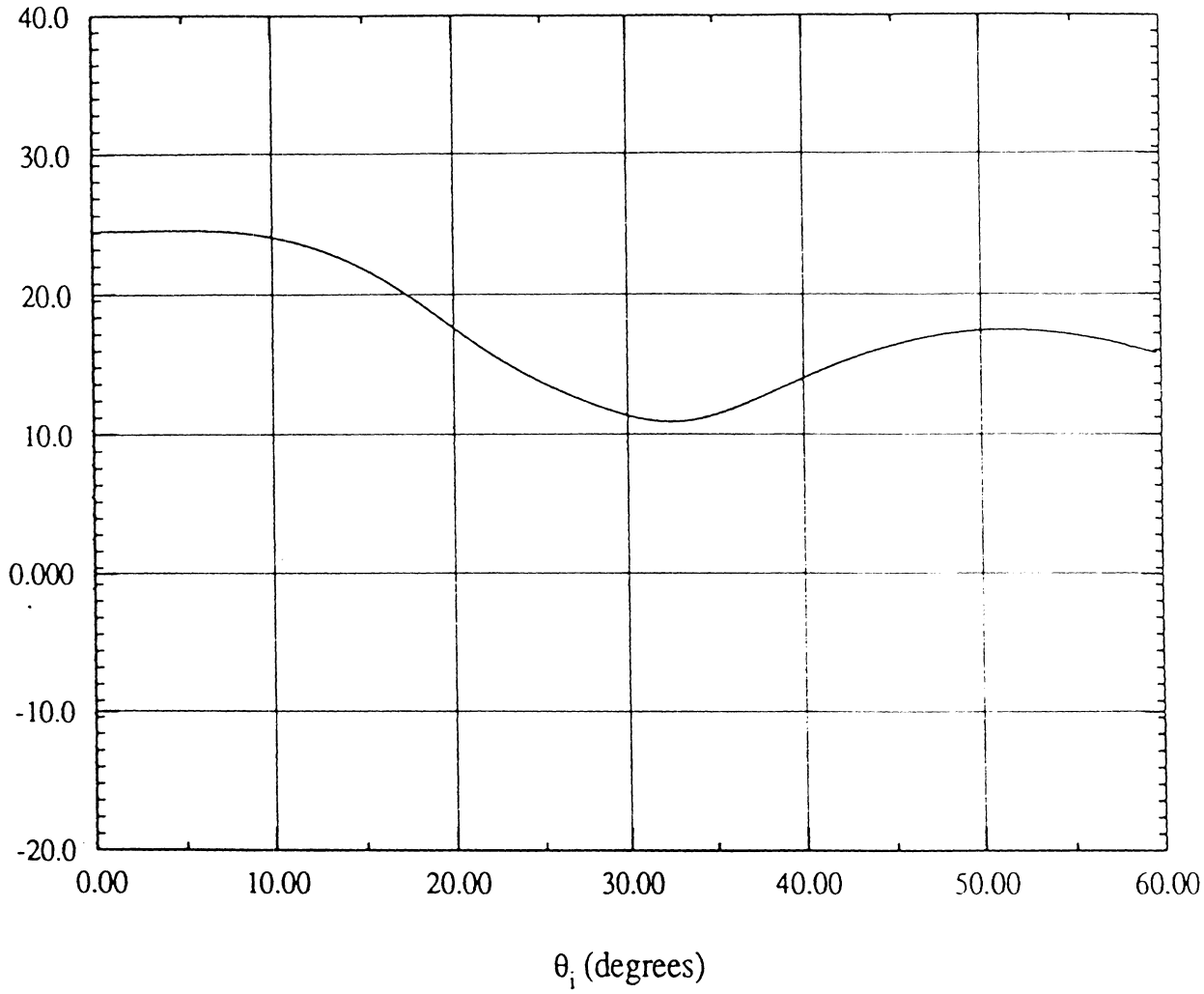

Figure 14: RCS (dB/λ^2) calculated by the Mode Matching Technique for a groove array termination with $a = 0.5\lambda, b = 1.5\lambda, l_1 = 5\lambda, l_2 = 0.2\lambda$, 4 fins, $\phi_w = 45^\circ, \phi_1 = 0^\circ$. (Vertical Polarization).

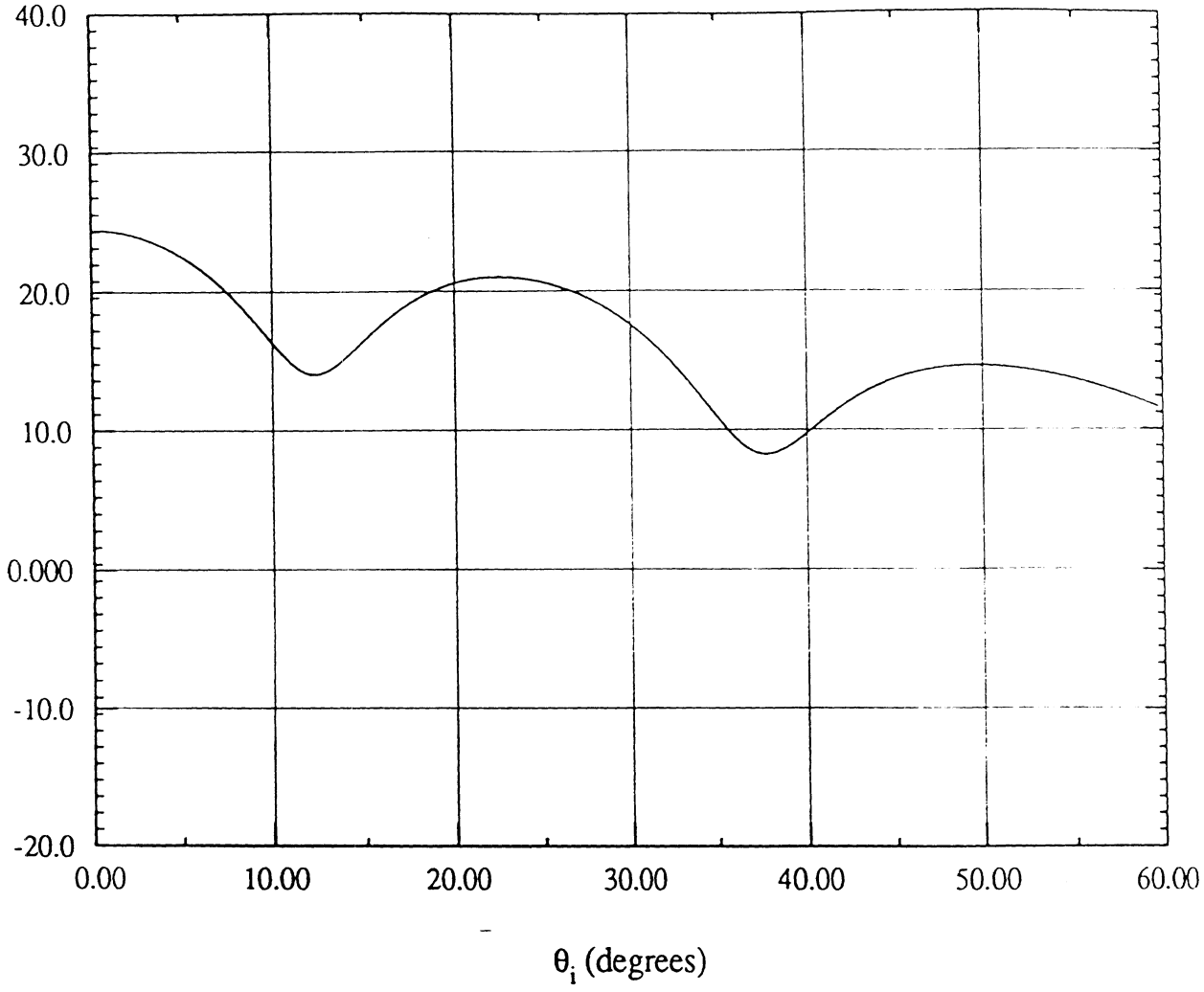

Figure 15: RCS (dB/λ^2) calculated by the Mode Matching Technique for a groove array termination with $a = 0.5\lambda, b = 1.5\lambda, l_1 = 5\lambda, l_2 = 0.2\lambda$, 4 fins, $\phi_w = 45^o, \phi_1 = 0^o$. (Horizontal Polarization).

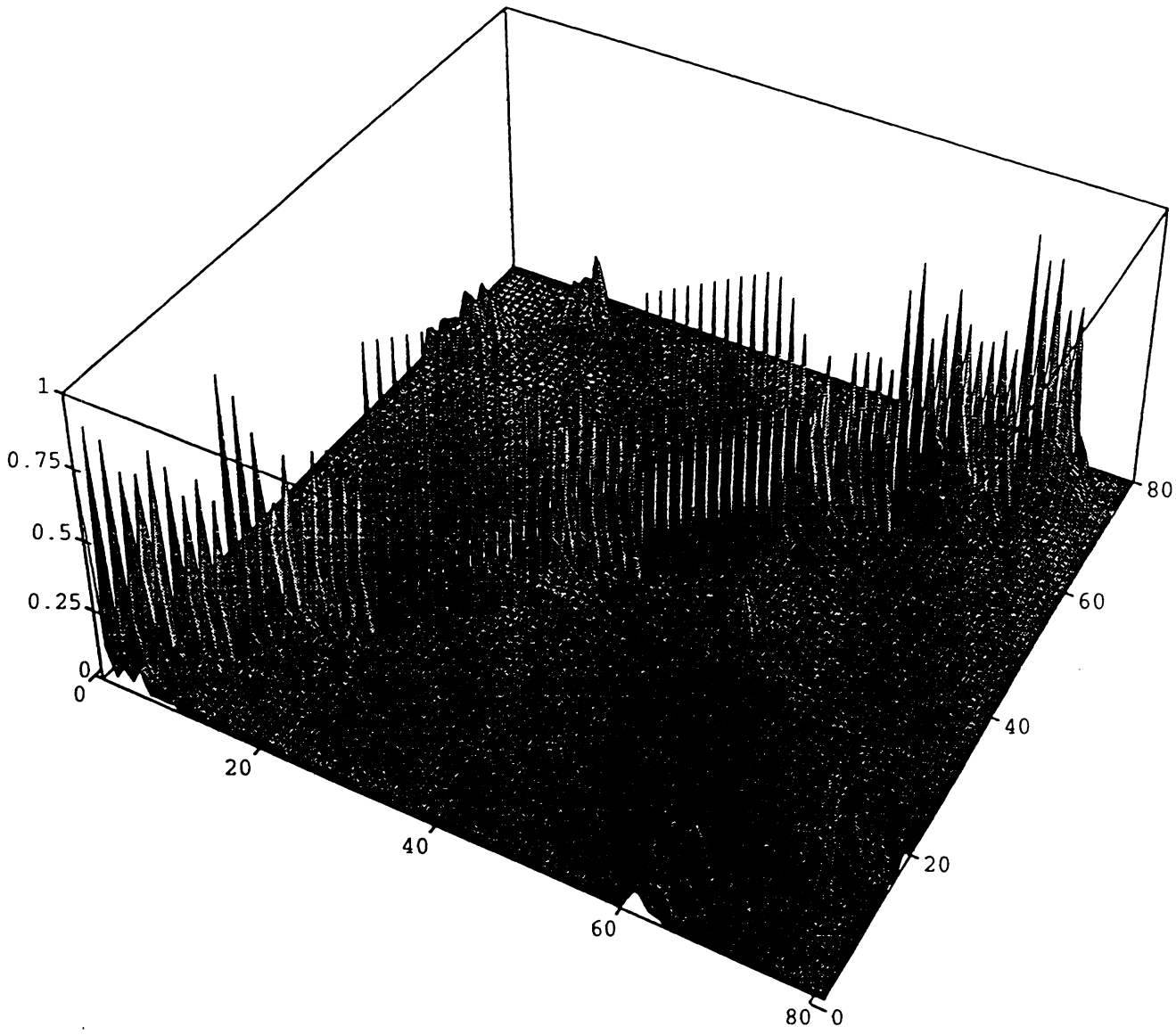

Figure 16: Amplitudes of the elements of the generalized scattering matrix calculated by Mode Matching for a groove array termination with $a = 1.5\lambda, b = 3\lambda, l_1 = 5\lambda, l_2 = 0.5\lambda, 8$ fins, $\phi_w = 40^o, \phi_1 = 10^o$. (See List of Figures for more details).

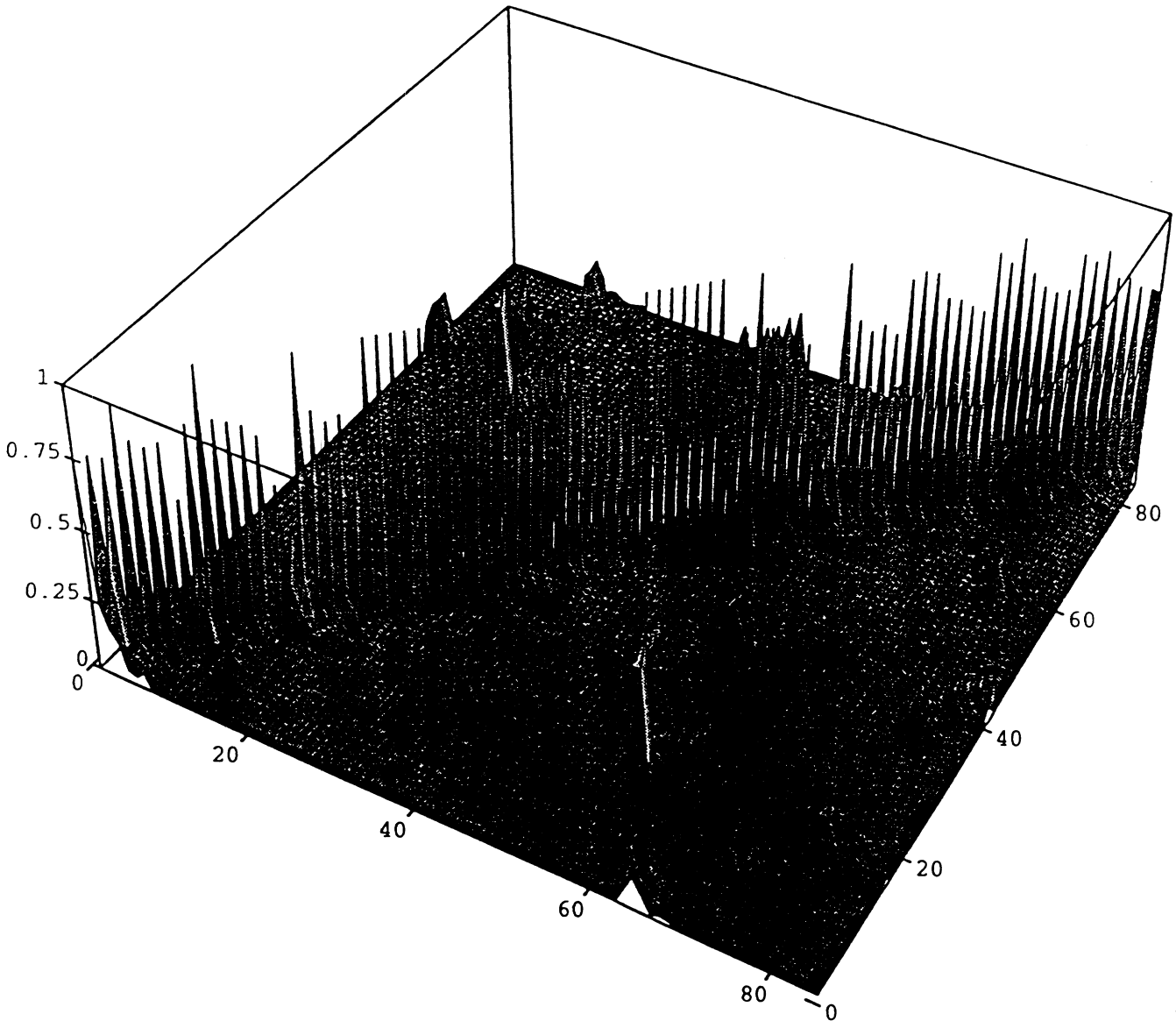

Figure 17: Amplitudes of the elements of the generalized scattering matrix calculated by Mode Matching for a groove array termination with $a = 0.5\lambda, b = 1.5\lambda, l_1 = 5\lambda, l_2 = 0.2\lambda, 4$ fins, $\phi_w = 45°, \phi_1 = 0°$. (See List of Figures for more details).

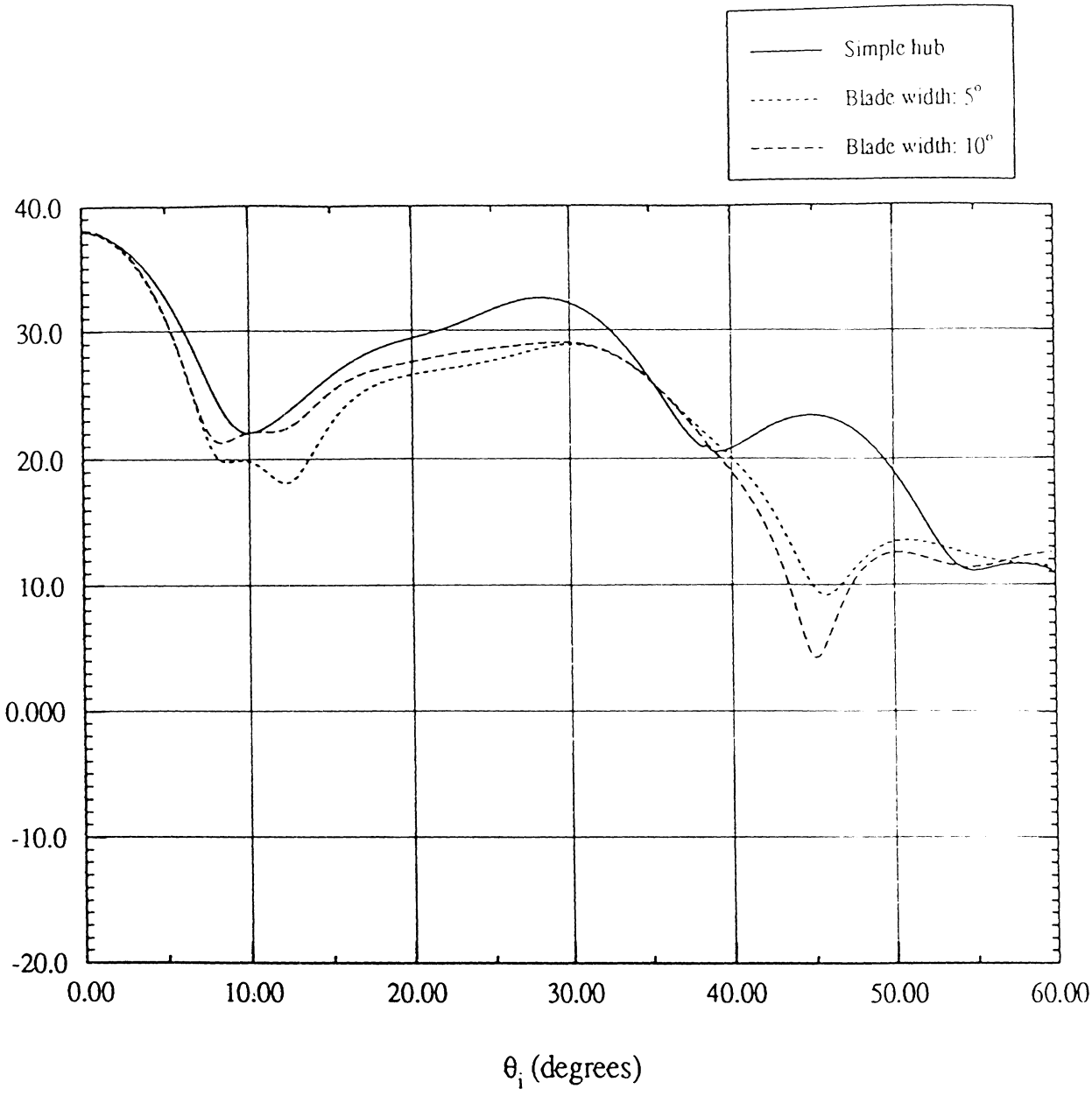

Figure 18: Effect of the presence of the termination blades on the RCS (measured in dB/λ^2). Dimensions: $a = 1.5\lambda, b = 3\lambda, l_1 = 5\lambda, l_2 = 0.5\lambda$, 8 blades, $\phi_1 = 0°$ (Vertical Polarization).

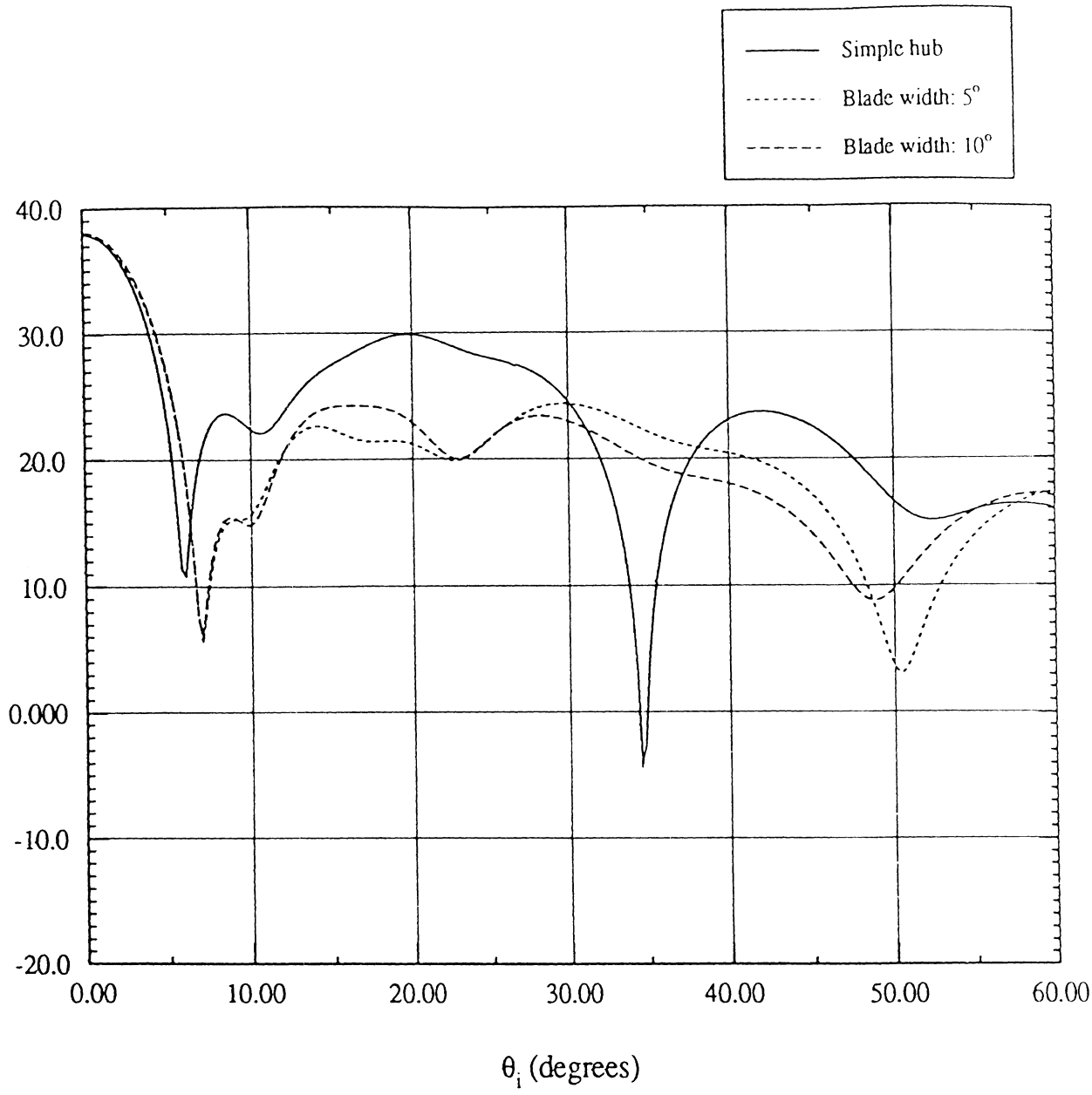

Figure 19: Effect of the presence of the termination blades on the RCS (measured in dB/λ^2). Dimensions: $a = 1.5\lambda, b = 3\lambda, l_1 = 5\lambda, l_2 = 0.5\lambda, 8$ blades, $\phi_1 = 0^\circ$ (Horizontal Polarization).